EXAMINATION OF THE REINFORCED CONCRETE SLAB STRUCTURE WITH BLOCK RAILS FOR TRAMWAY TRACK

E. KERKÁPOLY

Department of Railway Construction,
Technical University, H-1521 Budapest

Received October 10, 1985

Summary

On the track-slab structure with block rails introduced in 1972 on the tramway lines of Budapest, commission of the track building and operating as well as the r.c. track-slab producing institutions, the Department for Railway Construction of the Technical University of Budapest performed extensive research investigations. These investigations involved the theoretical determination of the different stresses generated in the block rails of the track structure, the examination of the ripple-building on the running surface and spinning over of this latter, the development of the insulated joints of the block rails, the detailed theoretical and laboratory test investigation of the r.c. track-slab, the stability examination of the assembled track structure, the laboratory-examination of the rail fastening, the design problems of foundation of the track, the vibration and noise measurements of the track and in the vehicles, the electrical measurements in the track and a great number of other technical problems of minor significance. The present study reports on the details and major results of a continuous, ten year's work and on the suggestions made for the development of the r.c. track-slab and block rail structure described in the paper.

Introduction

On the tramway lines of Budapest the track structure with r.c. track slabs and block rails has been first applied in 1972. The track structure in question is a new concept in so far as both of its system and structural design are concerned.

The Budapest Transport Co. which adopted the new system as well as the Concrete and Reinforced Concrete Industrial Works which manufactured the r.c. track slabs entrusted the Department of Railway Construction of the Technical University Budapest in 1974 and a new in 1980 with the research investigation on two different subjects which, however, related in essential to problems of the same track system. The objectives of the research investigation were to carry out theoretical and checking calculations for the evaluation of the stresses arising under the load and to perform field and laboratory tests for measuring the load-bearing capacity and to define the technical parameters of the track structure and its parts as well as to make suggestions with respect to the suppression of deficiencies observed during the operation.

The Department of Railway Construction has conducted during the last years the investigations according to the commission and made from the results

obtained ten final research investigation reports and thereafter, in 1982 summarized in a comprehensive study the results of the eight-year investigation work.

The Department of Railway Construction shares since then continuously in the development work of the new track system in question and in suppressing its deficiencies. This paper summarizes the theoretical and experimental investigations concerning the track system characterized by the r.c. track slab and block rails conducted at the Department of Railway Construction of the Technical University of Budapest.

1. Technical parameters of the track

1.1 The technical parameters of major significance

By way of preliminary, the technical parameters of major significance, the geometrical and material characteristics of the track system investigated and those of its elements should be presented.

The *standard cross section* of the track construction is depicted in Fig. 1 while Fig. 2 shows the structural parts to be found in the channel for the rail

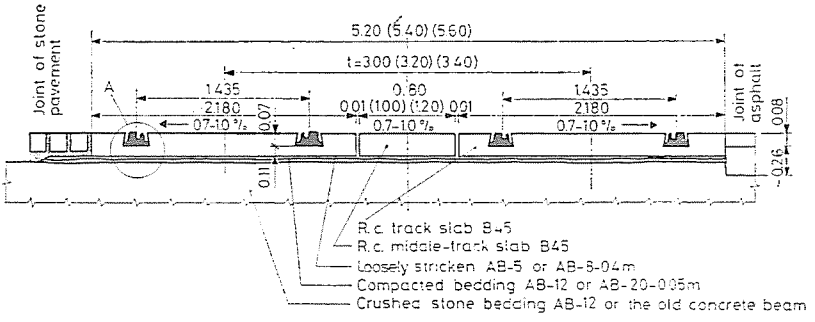

Fig. 1. Standard profile of the track

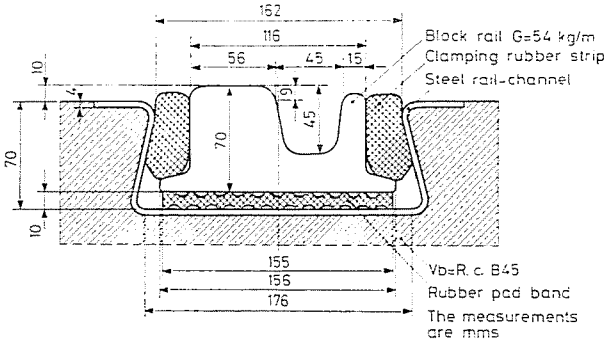

Fig. 2. Rail fastening

Table 1

Slabs fabricated from concrete B 450 made longitudinally with stressed, transversely with loose reinforcement. The slab VL-8 is made with loose reinforcement in both directions

Type	Effective length mm	Length taken into account in tangents for designing mm	Width	Mass kg/unit	Radius to be applied	
					horizontal	vertical
VL-60	5986	6000	2200	5530	>2000	>1200
VL-30	2903	2917	2200	2680	2000—550	1200—600
VL-15	1410	1424	2200	1300	550—150	600—200
VL-8	665	680	2200	620	150—40	
VK-60/8	5986	6000	780	2080	>300	>600
VK-30/8	2935	2950	780	1020	300—100	600—200
VK-15/8	1410	1424	780	490	100—40	
VK-60/10	5986	6000	980	2600	>300	>600
VK-30/10	2935	2950	980	1280	300—100	600—200
VK-15/10	1410	1424	980	610	100—40	

seat in the track slab. The *foundation* of the track structure is represented in case of a new track constructed along the trace of the preceding tramway line supported by the ballast or longitudinal concrete sleeper of the old track, while in case of a track laid on a new trace, according to the specification valid for the time being, a new ballast of crushed stone of a depth at least 30 cm should be laid.

As is shown in Fig. 1, a *solidified asphalt concrete bed*, over this a *loosely stricken asphalt bedding layer* are placed. The study of the possibilities the improvement of these structural elements is to be found in paragraph 4.5 of the present paper. The measurements of major significance of the r.c. track slabs are presented in Table 1. Figure 3 shows the drawing of the block rail whose parameters are presented in Table 2.

Figure 4 represents the expanding device for the block-rail track system which, if need be, should be arranged in the middle of the slab track type VL-60. The arrangement of the return-current cable at the expansion rail joints is shown by Fig. 5. In Fig. 6 the tensioning rubber strip and in Fig. 7 the details of the rubber pad applied under the block rail are represented.

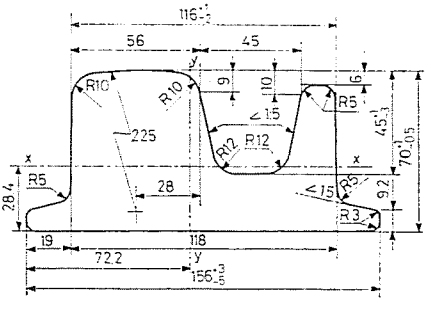

Fig. 3. The block rail

Table 2

Characteristic data	E N/mm²	G kg/m	T mm²	l m	I_z mm⁴
Calculated	215 000	52.75	6720	14 ± 0.002	$261.637 \cdot 10^4$

Characteristic data	I_y mm⁴	K_z mm³	K_y mm³	i_z mm	i_y mm
Calculated	$974.166 \cdot 10^4$	$62.88 \cdot 10^3$	$116.3 \cdot 10^3$	19.77	38.00

E = cross-section modulus
G = mass calculated
T = area of cross section calculated
l = length of rail
I_x, I_y = moments of inertia calculated
K_x, K_y = cross-section coefficients calculated
i_x, i_y = radii of gyration calculated

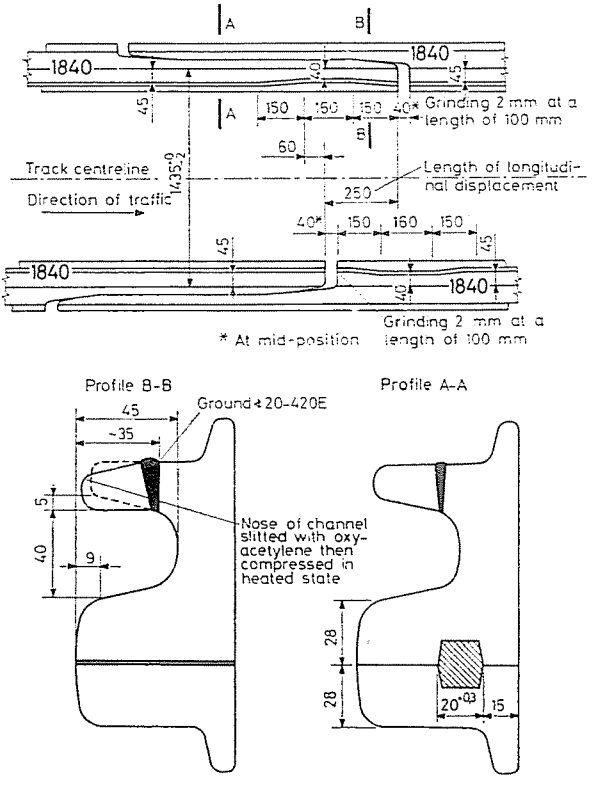

Fig. 4. **Expansion rail joint**

The longitudinal gaps between the concrete track slabs and the transverse gaps between the shorter track slabs applied in curved sections should be sealed with lean cement grout to 4—5cm depth.

The longitudinal gaps in their upper parts, the cross gaps to their whole depth (except those in the curved sections) as well as the lifting openings should be sealed by using bituminous rubber. Instead of the bituminous rubber all other impermeable elastic fillers might be used to this purpose.

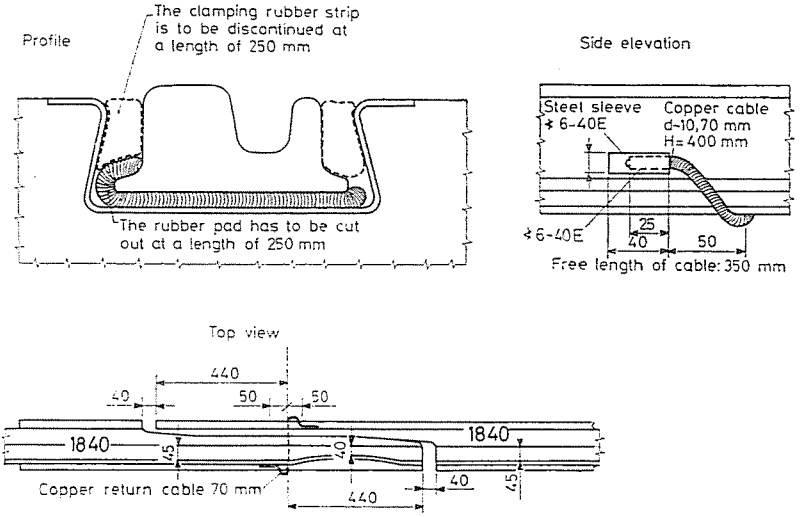

Fig. 5. Rail bond for the expansion rail joint

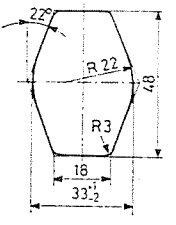

Fig. 6. Fastening rubber strip

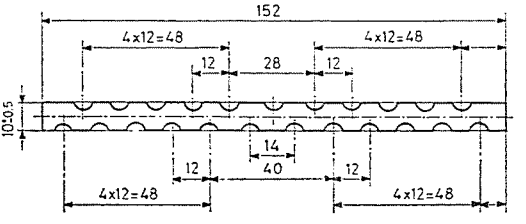

Fig. 7. Rubber pad

Table 3

Material			Material demand per track metre								
Naming	Number of nomenclature	Unit	$R_V > 2600$ $R_f > 1000$			$2600 > R_V > 300$ $R_f > 1000$			$300 > R_V > 40$ $R_f < 1000$		
			t = 0	t = 3.0	t = 3.2	t = 0	t = 3.0	t = 3.2	t = 0	t = 3.0	t = 3.2
AB-12		kg	1540	1820	1960	1540	1820	1960	1540	1820	1960
AB-5		kg	1121	1269	1316	1121	1269	1316	1121	1269	1316
VL-60	166-291-0112	pc	0.1667	0.1667	0.1667	—	—	—	—	—	—
VL-15		pc	—	—	—	0.7022	0.7022	0.7022	—	—	—
VL-8	166-291-0113	pc	—	—	—	—	—	—	1.4286	1.4286	1.4286
VK-60/8	166-291-0114	pc	—	0.0833	—	—	0.833	—	—	—	—
VK-60/10	166-291-0201	pc	—	—	0.0833	—	—	0.0833	—	—	—
VK-15/8		pc	—	—	—	—	—	—	—	—	—
VK-15/10		pc	—	—	—	—	—	—	—	—	—
Rubber pad	565-422-0090	m	2.04	2.04	2.04	2.04	2.04	2.04	2.04	2.04	2.04
Clamping rubber strip	565-514-1101	m	3.26	3.26	3.26	3.26	3.26	3.26	3.26	3.26	3.26
Block rail	216-114-0004	m	2.0	2.0	2.0	2.0	2.0	2.0	2.0	2.0	2.0
Channel for rail connecting cables	216-113-3660	pc	0.0208	—	—	0.0208	—	—	0.0208	—	—
Channel for track connecting cables	216-113-3660	pc	—	0.0104	0.0104	—	0.0104	0.0104	—	0.0104	0.0104
Cement } sand	138-211-0001	m^3	—	0.0033	0.0033	0.0155	0.0185	0.0185	0.0155	0.0155	0.0155
grout } C-45	151-110-0500	kg	—	0.0147	0.0147	0.0690	0.0823	0.0823	0.0690	0.0690	0.0690
Steel plate	252-715-0101	pc	—	0.3333	0.3333	—	0.3333	0.3333	—	0.3333	0.3333
Rubber bitumen	552-371-0001	kg	1.40	2.29	2.31	3.97	5.07	5.12	3.97	3.97	3.97
Electrode EB-1		kg	0.12	0.12	0.12	0.12	0.12	0.12	0.12	0.12	0.12
Electrode EB-200		kg	0.022	0.022	0.022	0.022	0.022	0.022	0.022	0.022	0.022

1.2 The tracklaying technique

During the research investigation conducted at the Department of Railway Construction the track laying technique of the r.c. slab-superstructure with block rails has been studied in detail and within this:

— the norms of the material,
— the specification concerning the temperature conditions during the tracklaying process,
— the specification concerning the processes of each of the tracklaying working elements, storing of the structural parts, preliminary operations, dismantling of the old track structure, welding of the block rail laying of the directive rails, preparation of the solid and loose bed layers, laying the rubber pads and block rails drawing in the fastening rubber strips, laying the mid-track slabs, designing the joining of the road pavements, sealing the slab joints and other accessory works.

In this paper the short repetition of the subject matter of the research work is unnecessary, however, for information, in Table 3 the materials required for laying a track with reinforced concrete track slabs and block rails in 1 km length are listed.

2. Examination of the block rails

2.1 Determination and evaluation of the stresses induced in the block rail

2.1.1 *Theoretical basis of the stress examination*

In connection with the stresses arising at the particular points of the block rail cross section, to be seen in Fig. 8, the following statements can be made.

The stress arising at *point 1* is generated by the bending effect of the wheel load Z, and also by the expansion stress, as well as by the internal stresses of the rail material. As a matter of course, all of the above stresses are arising at point 1 under every wheel passing over this point, consequently, to avoid the fatigue failure their resultant stress must not surpass the permissible fatigue strength.

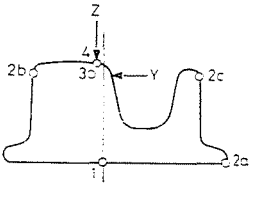

Fig. 8. Places of the stresses

Table 4

Stress		1	2a	2b	2c	3	4
Permanent							
Production stress	σ_{gy}	×	×	×	×		
Heat expansion stress	σ_t	×	×	×	×		
Stresses in curves	σ_R		×	×	×		
Z — bending	σ_{hx}	×	×	×	×		
Y — bending	σ_{hy}		×	×	×		
Z, Y — torsion	σ_{cs}		×	×	×		
Hertzian stress	σ_{Hertz}						×
Shear stress	$\tau_{\max}$					×	

The stress generated at *points 2a, 2b and 2c* is composed of the bending stress caused by the wheel load Z and the effect of the bending stress caused by the lateral force U, the bending effect of the rails forced into the curved sections of the track, as well as of the stresses detailed above. Particularly in the exterior fibres of the rail flange stresses might occur which may be higher than the yield strength causing by that plastic deformation.

At *point 3*, under the effect of the high concentrated wheel load, in a depth about 5 to 7 mm under the contact surface of the rail and wheel a shear stress might arise whose value might surpass the fatigue strength of the rail material and can cause pittings in the rail surface.

At *point 4*, point of application of the wheel load Z on the contact surface of the wheel and rail the so-called Hertzian tangential or contact stress is created.

The effects of stresses arisen at each of the above points are summarized in Table 4.

2.1.2 *Loading and track bedding data*

From among the types of vehicle GANZ UV-5, GANZ Industrial articulated and TATRA T-5, the type GANZ UV-5 representing the critical load has been selected as a basis for the calculations.

The value of the subgrade coefficient of the rail lying on continuous elastic support has been evaluated by taking Fig. 9 into consideration plotted on the basis of the test results demonstrating the elasticity of the support and that of the rail fastening elements by the relationship

$$D = \frac{P}{y} \quad \text{and} \quad C = \frac{D}{A},$$

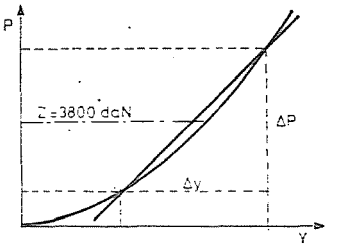

Fig. 9. Elasticity of the rail support

wherein A is the area of the loading platen used for the tests. In case of a single-layer rubber pad

$$C = 95 \text{ daN/cm}^3 .$$

The stresses to be seen in Table 4 have been successively defined.

2.1.3 *Permanent stresses*

a. *Manufacturing or internal stress* (σ_{gy})

The value of the stress σ_{gy} has been defined on the basis of the pertinent professional literature and the railway practice

$$\sigma_{gy} = 600 \text{ daN/cm}^2 .$$

b. *Expansion or thermal stress*

The value of the thermal stress may easily be defined by the commonly known theory in taking for basis the rail temperature variation $\Delta t = 50$ °C.

$$\sigma_t = \alpha E \Delta t = 1236 \text{ daN/cm}^2$$

c. *Rail stress caused by laying rails in curved tracks* (σ_R).

The value of this type of stress is given by the relation $\sigma_R = \frac{Ee}{R}$, the highest numerical value of which is, by taking the minimum radius $R_{\min} = 40$ m occurring on tramway lines for basis,

$$\sigma_R = 4504 \text{ daN/cm}^2$$

2.1.4 *Stresses depending on the gross weights of vehicles*

Since the block rail is supported by the rubber pad and the rubber strip in vertical and horizontal senses, respectively, in an elastic way, it seems to be convenient to proceed from the Zimmermann calculation method based on

substituting longitudinal sleeper complemented by the theory of professor Eisenmann in taking into account the scatter of the measurement results with the aid of the theory of probability.

a. *The bending stress generated by the vertical wheel load Z*

The final results of the detailed calculations are as follows:

— The value of the bending moment calculated with the Zimmermann method is

$$\boxed{\overline{M}_x = \frac{ZL}{4} \Sigma \mu}$$

wherein:

$$L = \sqrt[4]{\frac{4EJ}{Cs}}.$$

— The critical moment is:

$$M_x = \overline{M}_x \cdot \beta$$

wherein: $\beta = 1 + 3\,\bar{s}$.

— The critical stress is:

$$\sigma_{hx} = \frac{M_x}{K_x}$$

wherein K_x is the moment of resistance of the points examined of the rail cross-section about the x-axis.

The tensile stress at point 1 shown in Fig. 8 is:

$$\sigma_{hx} \cong 584 \text{ daN/cm}^2.$$

For information Table 5 indicates the maximum direct stresses originating from the bending effect of the vertical wheel load deduced for some tramway and main railway lines calculated from wheel loads occurring the most frequently.

In the table is to be seen that although the compressive stresses arising in the block rail under the effect of the vertical wheel load surpass the stresses of this type occurring in the tramway rails of the system *Phönix* but are not significantly higher than those generated in the main line rails:

$$\boxed{\sigma = \frac{ZL}{4K}[\Sigma \mu]\,\beta}.$$

Table 5

		Tramway track				State Railway track	
		Block rail incorporated in panel	Rail, type Phoenix, on crushed stone bedding	Rail, type Phoenix, on half-stiff support	Vignol-rail (48.5 kg/m) glued to r.c slab (KC-330)	Vignol-rail (48.5 kg/m) on wood slepper, and crushed stone bedding	Vignol-rail (UIC 54) on r.c slepper and crushed stone bedding
C	[daN/cm³[	95.24	8.0	—	—	—	—
s_0	[cm]	15.6	18.0	—	—	—	—
D	[daN/cm]	—	—	91 875.00	145 000	50 000	84 000
k	[cm]	—	—	122.5	66.6	77.0	60.0
U	[daN/cm³]	1 485.74	144.0	750	2 177.18	649.35	1 400.00
I_x	[cm⁴]	261.64	3 300	3 300	1 747	1 747	2 346
EI_x	[daNcm²]	$0.58 \cdot 10^9$	$7.10 \cdot 10^9$	$7.10 \cdot 10^9$	$3.76 \cdot 10^9$	$3.76 \cdot 10^9$	$5.04 \cdot 10^9$
L	[cm]	35.08	118.48	78.43	51.25	69.36	61.61
Z	[daN]	3 800	3 800	3 800	3 800	8 000	8 000
M	[daNcm]	53 790.83	180 089.60	119 213.60	77 900.00	221 952.00	197 152.00
K_{xf}	[cm³]	62.89	391.46	391.46	234.91	234.91	279.19
K_{xa}	[cm³]	92.13	344.83	344.83	237.26	237.26	312.92
σ_f	[daN/cm²]	855.32	460.05	304.54	331.62	944.84	706.16
σ_a	[daN/cm²]	583.86	522.26	345.72	328.33	935.48	630.04

b. *Bending stresses induced by the horizontal wheel load (Y)*

According to the calculations performed by following the principles given in the preceding paragraph we have:

$$\sigma_{hy} = \frac{M_y}{K_y} .$$

At *point 2a* of Fig. 8 one obtains

$$\sigma_{hy} = -796 \text{ daN/cm}^2 .$$

c. *Torsional stress arising under the effect of the vertical and horizontal wheel loads*

According to the theoretical and experimental examinations the lengths of the rail borders parallel to the longitudinal rail axis remain practically unchanged, wherefore, the normal torsional stresses might be neglected ($\sigma_{cs} = 0$).

d. *The critical stresses arising in the block rail*

— The critical stress generated at point 1 is:

$$\boxed{\sigma_{M1} = \sigma_{gy} + \sigma_t + \sigma_Z} ,$$

$$\sigma_{M1} = 600 \pm 1240 + 584 =$$
$$= +2424 \text{ daN/cm}^2 > \sigma_{H \text{ fatigue}} = 2300 \text{ daN/cm}^2 .$$

The fatigue strength of the rail material is:
2300 daN/cm² at a tensile strength 7000 daN/cm²
2550 daN/cm² at a tensile strength 8000 daN/cm²
2880 daN/cm² at a tensile strength 9000 daN/cm²

— The critical stress induced at point 2 is:

$$\boxed{\sigma_{M2i} = \sigma_{gy} + \sigma_t + \sigma_Z + \sigma_y} ,$$

$$\sigma_{M2a} = 600 \pm 1240 \pm 4504 + 584 \ (-796) =$$
$$= +6928 \text{ daN/cm}^2 > \sigma_{H \text{ yield}} = +4550 \text{ daN/cm}^2 ,$$

$$\sigma_{M2b} = +600 \pm 1240 \pm 3376 - 773 + 496 =$$
$$= +4939 \text{ daN/cm}^2 > \sigma_{H \text{ yield}} = +4550 \text{ daN/cm}^2 ,$$

$$\sigma_{M2c} = (+600) \pm 1240 \pm 2752 \pm 773 \pm 606 =$$
$$= -5371 \text{ daN/cm}^2 > \sigma_{H \text{ yield}} = -4550 \text{ daN/cm}^2 .$$

The yield strength of the rail material is:
4550 daN/cm² for a rail of tensile strength 7000 daN/cm²
5200 daN/cm² for a rail of tensile strength 8000 daN/cm²
5850 daN/cm² for a rail of tensile strength 9000 daN/cm²

e. *Hertzian contact stress on the contact surface of the wheel and rail*

In the neighbourhood of point 4 of the block rail (see Fig. 3) the railhead might be deformed under the pressure of the tyre of the wheel. The average value of the contact stress under the running wheels is

$$\boxed{\sigma = 435.16 \sqrt{\frac{\alpha Z}{R}}}$$

— the speed factor is:

$$\alpha = 1 + \frac{V^2}{30\,000} = 1 + \frac{60^2}{30\,000} = 1.12$$

— the weight of the wheel is:

$$Z = 3800 \text{ daN}$$

— the wheel radius is:

$$R = 33.5 \text{ cm},$$

thus,

$$\sigma = 435.16 \sqrt{\frac{1.12 \cdot 3800}{33.5}} =$$

$$= \underline{4904.87 \text{ daN/cm}^2 > \sigma_{H \text{ yield}} = 4550 \text{ daN/cm}^2}.$$

As is to be seen, the Hertzian contact stress is higher than the ultimate yield stress of the rail. However, as far as the elliptical contact surface does not touch the edge of the rail, the stresses higher than the yield strength have no particular influence on the durability of the rail, since the surfaces affected by the overburden are embedded between the particles of the rail steel recieving less load and thus they cannot evade under the pressure.

Due to the comparatively high value of the contact stresses arising between the wheel and rail it would be convenient to increase the critical tensile strength up to 8000 daN/cm². In this case the Hertzian pressure value would be $\sigma_{\text{Hertz}} = 4905$ daN/cm², less than the $\sigma_{H \text{ yield}} = 5200$ daN/cm².

f. *Shear stresses arising in the rail head*

In case where the stress under the repeated load of the wheel Z would surpass the fatigue strength of the rail steel, fatigue failure and pittings on the rail head would occur. The failure takes its beginning in the proximity of the contact surface of the wheel and the rail, in a depth 5 to 7 mm under it, and the significant shear stress might be considered responsible for the failure.

By knowing the value of the Hertzian stress induced on the contact surface of the wheel and the rail, the highest value of the shear stress arising in the

rail head might be evaluated:

$$\tau_{max} = 130.6 \sqrt{\frac{\alpha Z}{R}}$$

wherein:
— the speed factor is $\alpha = 1.12$,
— the wheel load is $Z = 3800$ daN,
— the radius of the wheel $R = 33.5$ cm,

$$\tau_{max} = 130.6 \sqrt{\frac{1.12 \cdot 3800}{33.5}} = 1472.05 \cong 1472 \text{ daN/cm}^2 .$$

The permissible value of the shear stress is:

$$\tau_{perm} = \frac{0.5}{\sqrt{3}} \sigma_{tens} \frac{1}{n}$$

wherein:

n — coefficient of reliability, equal to 1.1

$$\sigma_{tens} = 7000 \text{ daN/cm}^2$$

$$\tau_{perm} = \frac{0.5}{\sqrt{3}} 7000 \frac{1}{1.1} = 1837.02 \text{ daN/cm}^2 ,$$

i.e.

$$\tau_{max} = 1472.05 \text{ daN/cm}^2 < \tau_{perm} = 1837.02 \text{ daN/cm}^2 .$$

Under the traffic the hardening of the railhead surface may take place, which may result in the change of the contact stress and, according to the measurements, in the increase by 50 per cent of the stresses (the Hertzian surface pressure stress and the stress in the railhead). The hardened layer may cause in this way in the long run a premature pitting in the railhead.

Since the lubrication of the rails applied to reduce the wear of them also fosters the hardening of the railhead, in considering the fatigue failures also this negative effect of the lubrication should be taken into account.

2.1.5 *The evaluation of the permissible wheel load, i.e. wheel pressure from the point of view of the fatigue failure*

With knowledge of the maximum, i.e. permissible shear stresses in the railhead, for the value of the permissible wheel load and the permissible wheel radius the following relationships are obtained, respectively:

a)

$$\boxed{Z_{\text{perm}} = 5.26\ R\left(\frac{\sigma_{\text{tens}}}{\text{n}}\right)^2 10^{-6}}$$

and

b)

$$\boxed{R_{\text{perm}} = 1.9 \cdot 10^5\ Z\left(\frac{n}{\sigma_{\text{tens}}}\right)^2}\ .$$

The numerical data are as follows:

a) for the case of the wheel load:

— radius of the wheel, $R = 33.5$ cm,

— tensile strength, $\sigma_{\text{tens}} = 7000$ daN/cm^2

— safety, $n = 1.1$

$$Z_{\text{perm}} = 5.26 \cdot 33.5 \left(\frac{7000}{1.1}\right)^2 \cdot 10^{-6} = \underline{7135.78 \text{ daN} > Z_M = 3800 \text{ daN}}\ .$$

Such a value cannot occur but on sections carrying main-line trains.

b) for the case of the wheel radius:

— wheel load, $Z = 3800$ daN

— safety, $n = 1.1$

— tensile strength, $\sigma_{\text{tens}} = 7000$ daN/cm^2

$$R_{\text{perm}} = 1.9 \cdot 10^5 \cdot 3800 \left(\frac{1.1}{7000}\right)^2 = \underline{17.83 \text{ cm} < R = 33.5 \text{ cm}}\ .$$

Such a little wheel radius does not occur on tramways.

2.1.6 *Comparison of the rail profiles used by the tramway in Budapest, on the basis of the rail-quality parameters*

From the characteristics of the rails, six so-called coefficients of quality applicable in comparing the different rail profiles may be produced.

1. The moment of inertia (I_x) related to the weight of the rail per meter (g).

$$\boxed{\varepsilon_1 = \frac{I_x}{g}}$$

This coefficient characterizes the rail stiffness.

2. Ratio of the modulus of the rail profile (K_x) and the weight per meter of the rail which is characteristic to the load bearing capacity of the rail is:

$$\boxed{\varepsilon_2 = \frac{K_x}{g}}\ .$$

The track satisfies the requirements concerning the rail stiffness in case where the deflection of the rail is not significant and beyond this also the stress takes up favourable values. That is why the coefficients characterising the deflection (ε_3) and the stress (ε_4) are of significance in comparing the different rail profiles.

3.

$$\varepsilon_3 = \frac{100\,y}{\varepsilon_1}$$

wherein y is the magnitude of the rail deflection under the wheel load. This coefficient of the rail quality is characteristic to the rail stiffness.

4.

$$\varepsilon_4 = \frac{\sigma}{\varepsilon_2}$$

wherein σ is the maximum stress caused by the vertical wheel load.

The quality coefficients ε_5 and ε_6 give information concerning the capability of resisting to the dynamic impact forces of the rail cross section and rail material, respectively.

5.

$$\varepsilon_5 = \frac{A\,e}{K_x}$$

wherein

A — cross-sectional area,
e — distance of the extreme fibre,
K_x — section modulus with respect to axis intersecting the centre of gravity.

The lower the value of this coefficient, the better is the cross section of the rail exploited from the point of view of the dynamic effects.

6.

$$\varepsilon_6 = \frac{E\gamma}{\sigma_r^2}$$

wherein

E — Young's modulus of elasticity of rail steel,
γ — specific weight of rail steel,
σ_r — limit of elasticity.

This coefficient of quality is, as a matter of course, characterizing the material of the rail. The value of this expression also should be low, that is

Table 6

Quality coefficients of rail profiles used at the Budapest Transport Company (in case of supported by continuous rubber pad band)

		Rails				
		Block rails	Grooved rails NP-4	New 48	48.3	c
Parameters of rail profiles						
I_x	cm^4	261.64	3330.0	1747.0	1741.5	933.8
K_x	cm^3	62.89	348.0	235.0	235.1	145.2
A	cm^2	67.20	76.05	61.78	61.56	44.08
g	kg/m	54.01	59.7	48.5	48.3	34.5
γ	daN/cm^3	$7.85 \cdot 10^{-3}$	$7.85 \cdot 10^{-3}$	$7.85 \cdot 10^{-3}$	$7.85 \cdot 10^{-3}$	$7.85 \cdot 10^{-3}$
e	cm	4.16	9.57	7.43	7.41	6.43
y	cm	0.06	0.03	0.05	0.04	0.06
σ	daN/cm^2	855.31	279.23	389.44	389.02	558.59
Quality coefficients						
$\varepsilon_1 = I_x/g$		4.84	55.78	36.02	36.06	27.07
$\varepsilon_2 = K_x/g$		1.16	5.83	4.85	4.87	4.21
$\varepsilon_3 = 100\, y/\varepsilon_1$		1.24	0.05	0.14	0.11	0.22
$\varepsilon_4 = \sigma/\varepsilon_2$		737.34	47.90	80.30	79.88	132.68
$\varepsilon_5 = Fe/K_x$		4.55	2.09	1.95	1.94	1.95
$\varepsilon_6 = E\gamma/\sigma_r^2$		1.88	1.88	1.88	1.88	1.88

Note: $E = 2\ 150\ 000\ daN/cm^2$; $\sigma_r = 3000\ daN/cm^2$

why it is advantageous if for a lower specific weight, a high strength value is with the strain of the rail steel associated.

The values of quality coefficients of a few rail profiles are to be seen in Table 6. The numerical values are relative quantities, they are true only with respect to the rail systems investigated under identic circumstances. Thus, for example, in evaluating the quality coefficient ε_3 concerning the rail stiffness all of the rail systems have been investigated under the same bedding conditions, as continuously supported longitudinal beams.

A survey of the quality coefficients will be performed in the next paragraph in connection with the comprehensive evaluation of the block rail.

2.1.7 *Comprehensive evaluation of the block rail from the point of view of stresses arising in it*

For a simple evaluation easy to survey, the critical stress values generated by a complexity of loads are summarized in Table 7.

The block rail of low stiffness (ε_1, ε_3) is, from the point of view of the load bearing capacity (ε_2, ε_4 and Table 5), a highly exploited structural element.

Table 7

Kind of stress		1	2a	2b	2c	3	4
Permanent							
production stress	σ_{gy}	+600	+600	+600	+600		
heat expansion stress	σ_t	±1240	±1240	±1240	±1240		
stresses in curves	σ_R		±4504	±3376	±2752		
Z — bending	σ_{hx}	+584	+584	−773	−773		
Y — bending	σ_{hy}		−796	+496	−606		
Z, Y — torsion	$\Delta\sigma_2$	0	0	0	0		
Design stress	σ_M	+2424	+6928	+4939	−5371		
Hertzian contact stress	σ_{Hertz}						4905
Shear stress	τ					1472	
Permissible limiting stress	σ_H	2300	4550	4550	4550		4550

The increase of the value of tensile strength of the block rail from 7000 daN/cm² to 8000 daN/cm² would increase the permissible ultimate stresses over the critical stresses.

In turn, from the viewpoint of processing the dynamic loadings (ε_5), the block rail, due to its large cross-sectional area, contains significant reserves. Processing of the dynamic after-effects is fostered also by the two-way elastic support bedding of the block rail.

The second rubber pad arranged under the worn rails, due to the higher elasticity, increases the stresses by about 10 per cent:

$$\frac{L_2}{L_1} = \sqrt[4]{\frac{C_1}{C_2}} = \sqrt[4]{\frac{95.24}{67.24}} = 1.09$$

Owing to the curves of small radii to be found frequently especially in tramway networks, the wear resistance of the rails is of paramount significance. The problem in question grows in importance considering the necessity to hinder the wheels to run on the rail channel.

In comparing the relevant Hungarian norm with the material composition recommended by the UIC for steel rails, the very low content in Mn becomes immediately conspicuous which is one of the reasons for the unfavourable wear resistance of the rails produced in Hungary.

2.2 Corrugation of the block rail

Two types of examination have been carried out concerning the rail corrugation:

According to *Sztrókay* the occurrence of corrugation is hardly to be ex-

pected between the limits

$$0.015 > \frac{y}{s} > 0.003$$

in case of a rail continuously supported.

The sag y has been evaluated by making use of Zimmermann's method used as above, while the width of the rail flange is given: $y = 0.06$ cm, $s = 15.6$ cm which gives

$$0.015 > \frac{0.06}{15.6} = 0.0038 > 0.003 .$$

As is to be seen, the corrugation of the block rail is not dangerous although the Sztrókay-value approximates the limit.

The investigation carried out by *taking the Hertzian stress into account* refers to the fact that growing the round-off radius of the railhead and the elasticity of the fastening rubber strips might decrease the probability of occurrence of the rail corrugation.

2.3. Phenomenon of the cold rolling of the block rail

Two reasons for squashing the surface layer of the rail head by the cold rolling effect of the wheels might be made responsible:

1. If the elliptical contact surface is created at the edge of the rail head and stresses are induced at this part of the surface, so the steel particles overstressed evade to the same direction horizontally.

2. On the surface of the rail head, the wheels of the vehicles, owing to the irregular movements and to the conicity of the tyre besides the pure rolling also skiddings occur both in longitudinal and lateral directions. Mainly the shear forces of lateral direction induced by the skids are responsible for squashing the rail head.

2.3.1 *Squashing of the rail head under the effect of the contact surface stress*

The contact stress evaluated in Chapter 2.1.4 induced by the running wheel reaches, by assuming an ellipse of 1.2 cm minor axis, 4905 daN/cm^2 which is higher than the yield stress of the rail, this being 4550 daN/cm^2. (Eisenmann, on the basis of his tests took for his formula $2b = 1{,}2$ cm which seems to be a quite resonable value.)

From among the stresses causing squashing of the rail head, this is the highest value in case of a vehicle and elasticity ratio. The lowest value is the yield stress of the steel of the rail, when the contact ellipse is situated near the

rail head and the metal particles are permitted to deviate. The measurements of this smallest ellipse can be evaluated as follows:

— the highest pressure arising on the contact surface might be evaluated by making use of the following relationship:

$$\sigma_0 = 0.418 \sqrt{\frac{\alpha ZE}{2b R}} \tag{1}$$

— the "volume" of the stress ellipsoid, written in two different forms is:

$$Z = \frac{1}{2}\left[\frac{4}{3} \cdot \pi 2a\, 2b\, \sigma_0\right] = \sigma_{\text{aver.}}\, 2a 2b \pi ,$$

from which the highest pressure:

$$\sigma_0 = 1.5\ \sigma_{\text{aver.}}$$

wherein

$$\sigma_{\text{aver.}} = \sigma_{\text{yield}} ,$$

wherefore, replacing the value

$$\sigma_0 = 1.5\ \sigma_{\text{yield}}$$

into the above relationship we have:

$$1.5\ \sigma_{\text{yield}} = 0.418 \sqrt{\frac{\alpha ZE}{2b R}} ,$$

— the axis of the load ellipse perpendicular to the rail axis:

$$2b = 0.0777 \frac{\alpha ZE}{R\, \sigma_{\text{yield}}}$$

wherein:

α = 1.12 — speed factor,

Z = 3 800 daN — vertical wheel load,

E = 2 150 000 daN/cm² — Young's modulus of elasticity of rail

σ_{yield} = 4550 daN/cm² — limit yield stress of rail;

$$2b = 0.0777 \frac{1.12 \cdot 3800 \cdot 2150000}{33.5 \cdot 4550} = \underline{1{,}03\ \text{cm}} ,$$

— the measurement of the load ellipse parallel to the rail axis is:

$$\boxed{2a = 3.04\sqrt{\frac{\alpha ZR}{E\,b}}}$$

$$2a = 3.04\sqrt{\frac{1.12 \cdot 3800 \cdot 33.5}{215\,0000 \cdot 1.03}} = \underline{0.77 \text{ cm}}$$

2.3.2 *Squashing of the railhead under the effect of the skid forces*

The value of the skid force is:

$$F = \alpha(Zf + Y)$$

wherein f is friction coefficient equal to 0.25—0.15.

In case where the skidding frictions also take place at the edge of the rail head, the metal particles loaded can start to deviate in the lateral direction.

In such cases, the load surface is equal to the contact ellipse of minimum surface:

$$A = 2a\ 2b\pi,$$

thus, the value of the shear stress is:

$$\boxed{\tau_{cs} = \frac{F}{A} = \frac{\alpha(Zf + Y)}{2a \cdot 2b \cdot \pi}}$$

wherein $\alpha = 1.12$,
$Z = 3800$ daN,
$f = 0.25$,
$Y = 3040$ daN (lateral force),
$2a = 0.77$ cm,
$2b = 1.03$ cm;

$$\tau_{cs} = \frac{1.12(3800 \cdot 0.25 + 3040)}{0.77 \cdot 1.03 \cdot 3.14} = \underline{1794.46 \text{ daN/cm}^2 \approx \tau_{\text{perm}} = 1837.02 \text{ daN/cm}^2.}$$

Accordingly, also the surface shear stresses can cause squashing of the rails.

The torsional effect of both of the vertical and horizontal wheel load have already been mentioned in Chapter 2.1.4. The block rail being fastened with the aid of binding elements, more elastic than those commonly utilized, suffers a slight twist round its longitudinal axis. The rubber pad is more compressed on the side of the rail head than at the edge of the guard lip part. At the same time, the rubber strip at the guard lip side permits also a slight vertical dis-

placement. Consequently, also in the inside parts of the rail head squashing begins to proceed with the lateral displacement of the metal particles under the continuous load repetition, so to say making up the edge part of the rail head. That is the reason why the block rails suffer an increased degree of squashing.

2.4 The possibility of designing an insulated block rail joint

2.4.1 *Requirements raised against the insulated rail joints*

The objective of applying insulated rail joints is to preclude the conduction between the joining rail ends of the electric current of the railway signalling equipment. Accordingly, the two most significant demands in connection with the insulated rail joints are the electrically perfect insulation of the joining track panels as well as to assure the equivalence from the point of view of the load bearing capacity of the insulated rail joint by applying approrpriate complementary structural parts, with the continuous track interrupted by the insulation.

The insulation qualities of the design of insulated joints required

— The insulation capacity of the insulating elements should not be reduced during the service life of the rail joint.
— The insulating parts specified should be easily available and inexpensive.
— In case of a slight but otherwise non permissible displacement of the structural parts, the insulating elements should satisfy their function of insulation.

The points of view of load bearing capacity in designing insulated rail joints

— The insulated rail joint construction must prevent the vertical and horizontal displacements of the rail ends due to the loading and expansion of the rails, and assure a continuous guiding of the vehicle.
— It should possess an appropriate stiffness to resist the vertical and horizontal bending effects.
— The attachments between the structural parts, i.e. track panels should be safe against slackening.
— The changes of the cross sections of the structural parts should be made with smooth transitions.
— The structural parts, as for their forms, measurements and material have to be producible and inexpensive.

According to the shaping of the rail ends the joints can be arranged as a) abutting, b) bevel or c) lap joints (Fig. 10).

In case *a*) the continuity of the rail is interrupted at the same cross section perpendicular to the rail axis. In case of the alternatives *b*) and *c*), as in joining

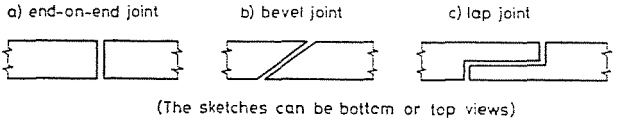

Fig. 10. Rail joints

of timbers, the rail ends are joint by "mortise and tenon". Further three possibilities offer here, according as the track panels, i.e. the rails are joint to each other with vertical, horizontal or varying planes.

2.4.2 *Basic respects of designing insulated block-rail joints*

In selecting the the design of the insulated block-rail joint, two ways, basically different, offer for the construction depending on whether the rail joint is to be arranged in the channel of the rail or, independently of the panel construction, in an independent track structure.

The principle of the longitudinal homogeneity of the railway track involves the requirement to endeavour, simultaneously with dividing the track slab structure into insulated sections, to design an-insulated joint which could be arranged in the track slab.

The room available for arranging the insulated block-rail joint in the channel of the slab with its structural parts (fish-plates, bolts) is strongly limited in the channel of the track slab, wherefore, the application of the voluminous fish-plates is to be avoided.

Using bolted, side fish-plates for but joints, if only because the drilling difficulties due to the low height of the block rails is hardly possible. A strong base fish-plate of significant moment of inertia might be arranged only by deepening the channel in the track slab, however, this expedient is not feasible owing to the thickness of the track slab of 18 cm, i.e. under the channel 11 cm.

Thus, the search for a convenient insulated lap joint design should be conducted towards a solution feasible by applying fish-plates of smaller measurements.

The cooperation of rails bound together along the horizontal plane (Fig. 11, variant *1*) is more favourable than of those bound along vertical plane (Fig. 11, variant *2*).

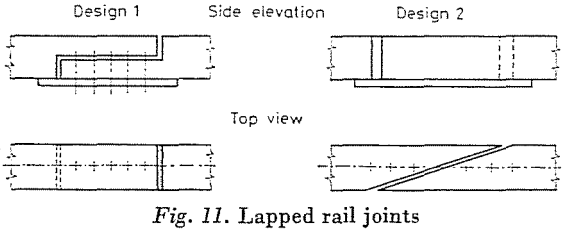

Fig. 11. Lapped rail joints

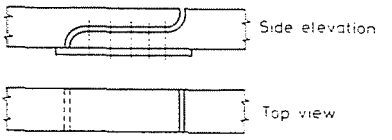

Fig. 12. Lapped rail joint

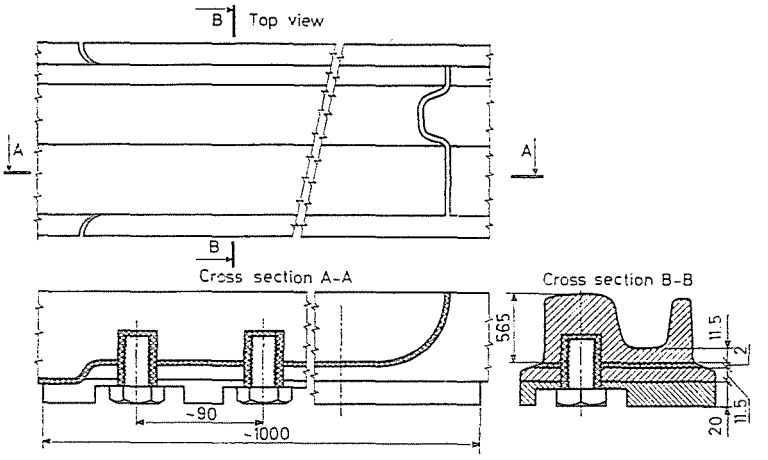

Fig. 13. Rail joint suggested, variation 1

In case of variant *1* the uniformity of the lack of the cross section can be realized by the lap joint of the vertical sections (Fig. 12).

The approximate geometry of the insulated joints of the block rails suggested by the Department is to be seen in Figs 13 and 14 in two elevations.

Variant 1 (Fig. 13)

The block-rails cut at a depth 11 mm, i.e. 14 mm under the rail groove are fitted to each other by lap joint. The expansive force is resisted by the bolts screwed in the vertical holes bored from the direction of the base into the rail body. The insulation is realized partly by the glass fibre put between the joining surfaces of high compressive strength, partly by the insulating rings put into holes. All the insulating elements are glued to the surfaces by epoxy resins.

Variant 2 (Fig. 14)

Between the rails cut askew along vertical planes as well as between the rail base and the fish-plates insulations made by the same techniques are arranged. The angle of inclination of the intersection formed with the rail axis is defined by the spacing of the bolts and by the principle of the continuous change of the cross section under the loading.

For both variants owing to the 15 mm thickness of the base fish-plate, a deeper channel than the usual is to be arranged in the track slab. Therefore,

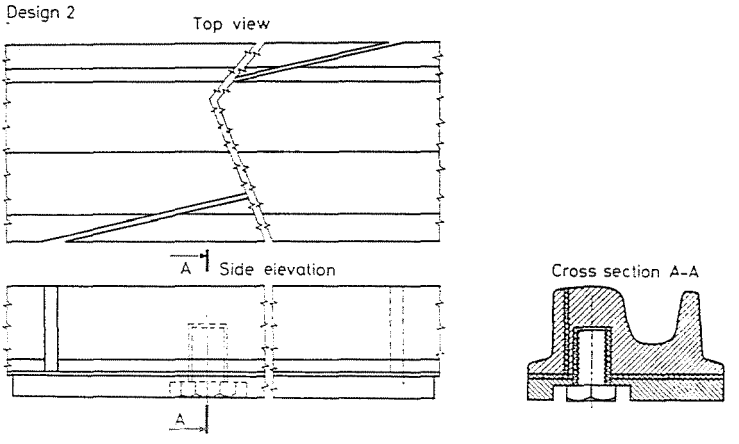

Fig. 14. Rail joint suggested, variation 2

the slabs supporting the insulated rail joint are presumably to be made thicker by 15 mm than those used under the uninterrupted rail. However, a definitive decision concerning this problem could only be made after the detailed structural design of the track slabs.

Also the approximate structural dimensioning of the insulated lap joints has been carried out by the Department. More other variants of the design of the insulated rail joints which, however, are here not detailed, have been worked out but, due to the relatively larger dimensions, they cannot be located into the usual channel which ought to be made deeper, i.e. a significantly stronger track slab should be constructed to support the insulated rail joints.

3. Examination of the r.c. track slab

3.1 Evaluation of the critical load, checking of slab strength

3.1.1 *Preliminaries*

In designing the r.c. track slabs, the following structural dimensioning procedures have been applied during the last 12 years which in carrying out the the examination of the track slab by the Department described below have also been taken into account:

I — Two-way tensioned slab designed by the Concrete and Reinforced Concrete Industrial Works (BVM) (1970)

II — Two-way slab tensioned along the longitudinal direction with untensioned reinforcement in the lateral direction (1971) designed by the BVM

Table 8

Sub-grade coef-ficient (N/mm)	No. of Drawing	Longitudinal bending moment				Transversal bending moment			
		M+		M−		M+		M−	
		Tramway	Road	Tramway	Road	Tramway	Road	Tramway	Road
C = 0.04									
	I.	55.4	—	−69.4	—	18.0	—	−11.3	—
	II.	57.7	38.6	−74.4	−93.6	15.8	39.2	0	−50.3
	III.	57.7	38.6	−74.4	−93.6	15.8	39.2	0	−50.3
	IV.	51.4	39.0	−75.9	−48.0	9.7	24.9	−13.6	−33.0
C = 0.075									
	V.	84.2	28.6	−102.5	−35.3	13.1	18.3	0	−25.2
C = 0.04									
	BME V.T.	59.4	68.4	−55.3	−38.8	20.1	27.0	−24.9	−19.3

III — Slab with two-way untensioned reinforcement designed by the State Company for Communication, Transport and Traffic Engineering, Planning and Design Services (UVATERV) (1974)

IV — Slab reinforced with longitudinal tensioned wires, i.e. strands and untensioned cross reinforcement designed by the UVATERV (1978)

V — Slab designs worked out by the BVM, i.e. by the Department for Railway Construction to foreign (Czecho-Slovakian, Swiss, Bularian and Dutch) orders constructed to loads other than those in Hungary (1978—1982).

All of these designing procedures are based on the model of the slab as a beam continuously supported on elastic bedding and the stresses induced are evaluated by different influence charts taken from the literature on the subject. The bending moments induced in the longitudinal and lateral directions show, as indicated in Table 8, a significant scatter. The reason for this is to be found in the approximate calculation of a beam model; in the neglect of the rail channel and in assuming the vehicle load as a concentrated force.

3.1.2 *Computer aided evaluation of critical stresses induced in the track slab*

3.1.2.1 *Basic data*

a. *Tram-car load* serving for basis of the calculation:
   — Axle arrangements and loads are to be seen in Fig. 15.
   — Design wheel-load is that of the vehicle type "A":

$$Z_M = Z_E(1 + ts) = 62.5(1 + 3 \cdot 0.2 \cdot 1.0) = 100\ kN$$

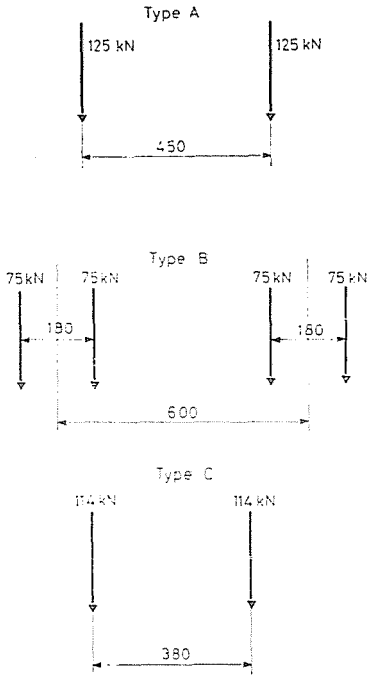

Fig. 15. Tramway axle load specified

b. *Road-vehicle* loading:
   — Vehicle types according to the Hungarian Regulation for Highway Bridges (Fig. 16).
   — Design wheel-load of the vehicle type "A" is

$$Z_M = \cdot k_e \cdot Z_E = 1.2 \cdot 1.1 \cdot 100 = 132\ kN$$

c. The value of the *coefficient of the subgrade reaction* is assumed on the basis of the examinations summarized by *Chapter 4.5* of the present paper as follows:

$$C = 0.04\ N/mm^3\ (= 4\ kp/cm^3).$$

3.1.2.2 *Method of calculation*

The evaluation of the stresses generated in the track slab had been carried out with the aid of a spatial grid model. For the solution of the computer program of a general spatial grid, the method of matrix displacement is to be applied.

Before preparing the data tape, a fictitious division ought to be carried out on the slab to make the model meet the program requirements. Along the axes of the individual prisms obtained by the longitudinal and cross division of the

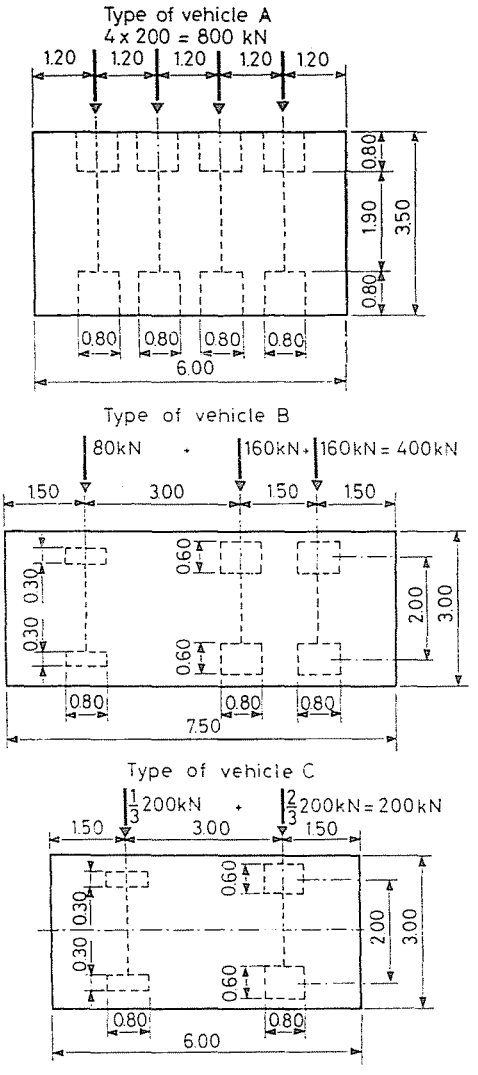

Fig. 16. Specified load for road pavements

slab one assumes bars which have the same cross-sectional characteristic data like those of the prisms. In this way, essentially, a grid, composed of bars and nodes is produced. The bars are of straight axes and of constant cross section, and the nodes are elastically a grid, composed of bars and nodes is produced. The bars are of straight axes and of constant cross section, and the nodes are elastically supported.

In dividing the track slab into prisms the following aspects had to be taken into consideration:

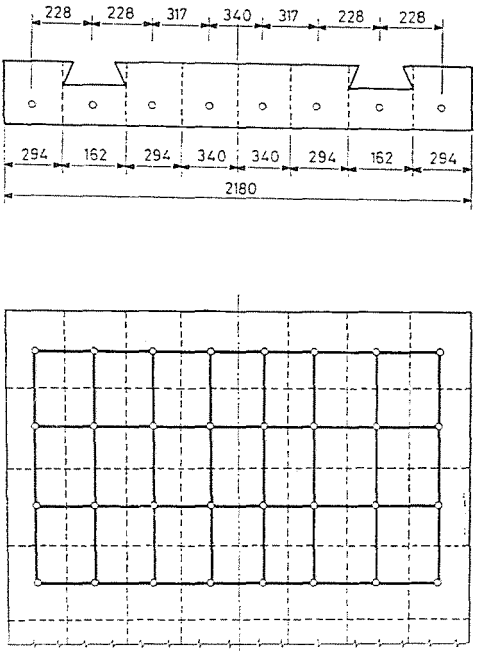

Fig. 17. Division of the track slab

— Due to the cuts formed by the channels for placing the rails, the thickness of the track slab is not uniform, wherefore, the height of the longitudinal and cross bars (i.e. prisms) differ from that of the grid bars lying at other parts of the slab.
— The ratio of the bar lengths to each other must not surpass the quotient 1 : 2.
— The forces working on the track slab can be applied only at the nodes of the grid, wherefore, the axlebases, i.e. the wheelbases also should be taken into account.
— The density of the division is only limited by the machine-available time.

By taking the above aspects into consideration, the division outlined in Figs 17 and 18 has been selected. The grid contains 120 nodes, 217 bars of 6 different types.

The input data of the program established by the Department of Mechanics according to the input sequence:
— number of nodes,
— number of bars,
— number of bars of different types,
— load data.

The elastic behaviour of the subgrade is represented by the spring constant D (N/mm) which has been evaluated from the subgrade coefficient

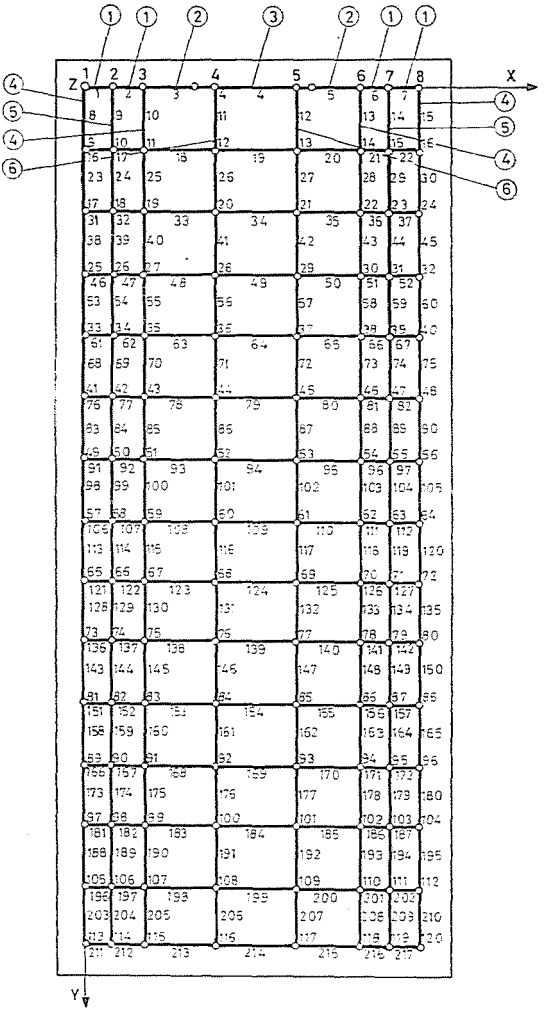

Fig. 18. Division of the track slab

C (N/mm^3) by making use of the formula

$$\boxed{D = C \cdot A}$$

wherein

A (mm^2) — surface area encircled by normal bisectors starting from node in question.

The critical load patterns of the tram-cars are to be seen in Fig. 19 and those of the road traffic in Fig. 20.

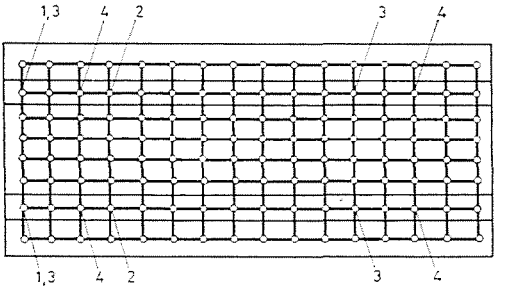

Fig. 19. Load pattern of tramway vehicle

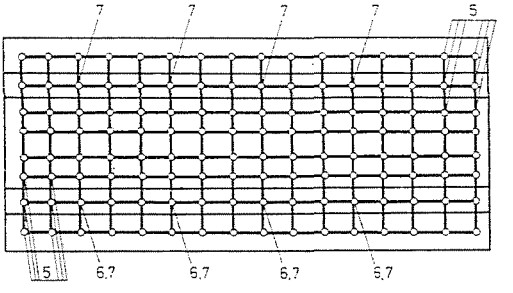

Fig. 20. Load pattern of road vehicle

Table 9

Load	No. of load pattern	No. of nodes loaded by concentrated force	Design bending moment in longitudinal direction		Design bending moment in transversal direction	
			M+ (mkN)	M− (mkN)	M+(mkN)	M− (mkN)
Tram-way	1	2, 7,	0.23/1.70	12.43/55.32	7.09/17.73	9.94/24.85
	2	34, 39,	13.36/59.41	2.09/15.49	8.03/20.08	6.37/15.93
	3	2, 7, 90, 95,	12.28/54.60	7.29/54.06	8.03/20.08	6.32/15.81
	4	18, 23, 106, 111,	11.91/52.95	1.94/14.40	8.05/20.13	6.90/17.26
Road	5	1, 2, 3, 9, 10, 11, 110, 111, 112, 118, 119,	2.12/15.75	4.43/32.85	0.79/1.98	2.44/6.09
	6	18, 42, 66, 90,	15.38/68.43	5.24/38.83	10.78/26.95	5.45/13.63
	7	18, 23, 42, 47, 66, 71, 90, 95,	14.02/62.35	0.08/0.59	10.13/25.33	7.71/19.28

Note: The values of the numerators concern the bending moments indicated in the bars, those in the denominator apply to the whole width of the slab in the longitudinal direction, and to a 1 m length of the slab in the cross direction.

After the run of the computer program one obtains as results the stresses induced at the bar ends (bending moments and shear forces) as well as the reaction components of the elastic supports.

The highest values of the longitudinal and cross bending moments associated with the different load patterns are summarized in Table 9.

3.1.3 *Checking of the track-slab strength*

3.1.3.1 *Checking of the longitudinal reinforcement*

a. *Geometrical and strength parameters of the reinforced concrete cross section*

The cross section of the track slab taken for basis is to be seen in Fig. 21. Calculation results:

— Distance of the median of the cross section
— from the top exterior fibre: $x_b' = 93.37$ mm
— from the bottom exterior fibre: $x_b = 86.63$ mm
— The moment of inertia of the concrete cross section with respect to its centroidal axis is:

$$I = 97\,767 \cdot 10^4 \text{ mm}^4$$

Distance of the median of the tension wires to the bottom exterior fibre is (Fig. 22):

$$x_v = 88.60 \text{ mm}$$

— Moment of inertia of the tension wires with respect to their own median is

$$I_v = 322.47 \cdot 10^4 \text{ mm}^4$$

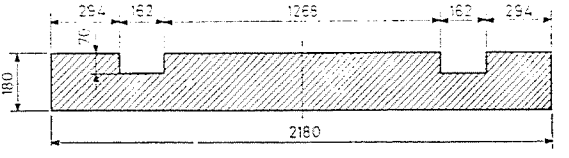

Fig. 21. Cross section of the track slab

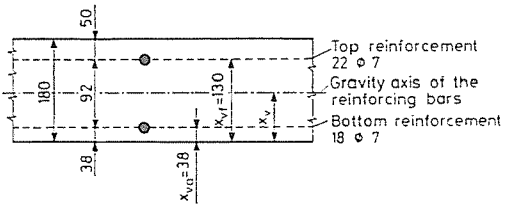

Fig. 22. Placing of the tensioning wires

— Percentage of the steel cross section with respect to the concrete cross section:

$$a = 0.4164\ \%.$$

b. *Examination concerning the first stress pattern*

— Coefficient of homogenization: $n_1 = 5.0$

— Ideal cross section of concrete:

$$F_{i1} = 375\,878\ \text{mm}^2$$

— Distance from the median of the ideal cross section of the concrete to the bottom exterior fibre:

$$x_{i1} = 86.66\ \text{mm}$$

— Moment of inertia of the ideal cross section of the concrete with respect to its own median:

$$I_{i1} = 99\,059 \cdot 10^4\ \text{mm}^4$$

— Moment of resistance of the ideal cross section of the concrete with respect to the bottom fibre:

$$K_{i2}^a = 11\,469 \cdot 10^3\ \text{mm}^3;$$

with respect to the top fibre:

$$K_{i1}^f = 10\,684 \cdot 10^3\ \text{mm}^3$$

— Loss of stress caused by slow deformation, i.e. relaxation:

$$\Delta\sigma_{v\,\text{rel}} = 165\ \text{N/mm}^2$$

— The effective tensioning stress of the tensioning wires:

$$\sigma_{v\,M1} = 915\ \text{N/mm}^2$$

— Eccentricity of the tensioning wires:

$$e_1 = 1.94\ \text{mm}$$

— The maximum eigenstresses at the application of tensioning
— in the bottom extreme fibre:

$$\sigma_{1a} = -3.51\ \text{N/mm}^2 < \sigma_{bH} = 20.5\ \text{N/mm}^2$$

— in the top extreme fibre

$$\sigma_{1f} = 4.01\ \text{N/mm}^2 < \sigma_{bH} = 20.5\ \text{N/mm}^2$$

c. *Examination in case of the third stress case*

— The modulus of deformation of the concrete in case of sustained loading

$$E_{b3} = 18\,143 \text{ N/mm}^2$$

The calculated values to be found under the above point b. are in the same sequence as follows:

$$n_3 = 10.5$$
$$F_{i3} = 2\,384\,344 \text{ mm}^2$$
$$x_{i3} = 86.70 \text{ mm}$$
$$I_{i3} = 100\,836 \cdot 10^4 \text{ mm}^4$$
$$K_{i3}^a = 11\,631 \cdot 10^3 \text{ mm}^3$$
$$K_{i3}^f = 10\,808 \cdot 10^3 \text{ mm}^3$$

— Loss of stress casued by shrinkage:

$$\sigma_{vzs} = 76 \text{ N/mm}^2$$
$$\sigma_{vM3} = 839 \text{ N/mm}^2$$
$$P_{f3} = 1\,291\,540 \text{ N}$$
$$e_3 = 1.90 \text{ mm}$$

— The stresses in the extreme fibres caused by the positive bending moment *inducing tensile stress at the bottom:*

$$\sigma_{3a} = 1.26 \text{ N/mm}^2 \quad < \quad \sigma_{hH} = 1.7 \text{ N/mm}^2$$
$$\sigma_{3f} = -8.34 \text{ N/mm}^2 \quad < \quad \sigma_{bH} = 20.5 \text{ N/mm}^2$$

— The stresses in the extreme fibres from the negative bending moment *inducing tensile stress at the top:*

$$\sigma_{3a} = -6.72 \text{ N/mm}^2 \quad < \quad \sigma_{bH} = -20.5 \text{ N/mm}^2$$
$$\sigma_{3f} = 0.25 \text{ N/mm}^2 \quad < \quad \sigma_{bH} = 1.7 \text{ N/mm}^2$$

d. *Determination of design bending moments*

— The positive design bending moment with respect to the bottom reinforcement is:

$$M_H^+ = 68.43 \text{ mkN}$$

— The negative design bending moment with respect to the bottom reinforcement is:

$$M_H^- = 55.32 \text{ mkN}$$

3.1.3.2 *Checking the transverse reinforcement*

a. *Examination of the concrete slab section of 180 mm thickness* (Fig. 23)

— Bottom reinforcement: $F_{vasz} = 550.67 \text{ mm}^2/\text{m} < F_{va} = 707 \text{ mm}^2/\text{m}$
— Top reinforcement: $F_{vfsz} = 513.85 \text{ mm}^2/\text{m} < F_{vf} = 707 \text{ mm}^2/\text{m}$

b. *Examination of the concrete slab section of 110 mm thickness under the rail channel* (Fig. 24)

— Bottom reinforcement: $F_{vasz} = 1149.26 \text{ mm}^2/\text{m} > F_{va} = 707 \text{ mm}^2/\text{m}$

As the calculation shows, the cross section of the bottom reinforcement in the concrete strip under the rail is not sufficient to resist the load. In this context, however, it is to be noted that the design bending moment is induced by the loading of the lorry wheel but the road vehicle transmits its loading in reality through the pneumatic of the wheel, on a surface at least of an area 0.25×0.80 m. However, in establishing the computer program the wheel loading of the vehicle is applied as a point load (except the case of the edge loading). For this reason, in the cross sections under the load, the stresses calculated in this way are higher than in reality.

In case, where the determination of the stresses induced in the track slab will be carried out in the future by assuming a model slab, the examination of both modes of load will be suggested.

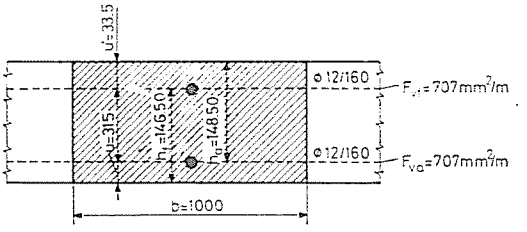

Fig. 23. Drawing for the examination of the cross reinforcement

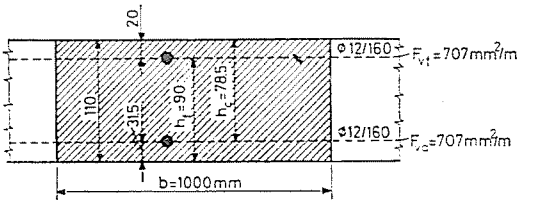

Fig. 24. Drawing for the examination of the cross reinforcement

3.1.3.3 *Examination of the width of cross cracks*

The cross reinforcement of the track slab is placed at the longitudinal centre line of the slab as is demonstrated in Fig. 25.

— Coefficient of homogenization: $n = 8.40$
— Thickness of compressed concrete: $x = 41.78$ mm
— Calculated stress in an extreme tensioned steel wire at stress pattern 2: $\sigma_{v2} = 186.21$ N/mm^2
— Moment of inertia of nominal concrete cross section: $I_i = 53\,799 \cdot 10^4$ mm^4
— Moment of inertia of concrete cross section of 1 m length with respect to its own median: $I_b = 48\,600 \cdot 10^4$ mm^4
— Moment of resistance of nominal concrete cross section: $K_i = 5978 \cdot 10^3$ mm^3
— Fictitious design stress in an exterior fibre to be calculated on basis of stress pattern 1: $\sigma_{b1} = 4.51$ N/mm^2
— design crack width: $a_M = 0.16$ mm $< a_H = 0.2$ mm

3.1.4 *Summary of the calculation*

After reviewing and evaluating the different ways dimensioning of the prefabricated r.c. track slab structure I suggested to change the process of designing. The two design basic elements — determination with the aid of the theory of probability of the design load and dimensioning as a slab of the concrete element by making use of the method of matrix displacement — serve for the approach of the actual stresses and stress patterns and, last of all, the economical and on the safety side designing. In considering the values of the design bending moments, it can be pointed out that the degree of utilization of the track slab VL-6 pretensioned, manufactured at present, considering the stresses in the exterior fibres is 35 to 75 per cent, the limiting bending moments 50 to 70 per cent and, on the basis of the bending tests 55 per cent.

Considering the issues of the research investigations I suggested to carry out the future design of track slabs by making use of the procedure of dimensioning exposed above.

3.2 Laboratory ultimate-strength test on track slab

3.2.1 *Test setup*

For the purpose of the static ultimate strength test a closed steel structure frame, shown in Figs 26 and 27 has been produced.

To the lower cross beams of the steel-structure frame load distributing elements are mounted on which a steel bar of 40×400 mm measurements is supported bearing the track slab along its longitudinal direction. Upon the top

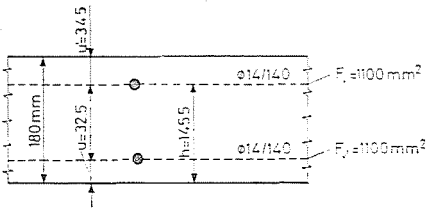

Fig. 25. Drawing for the examination of the width of cracks

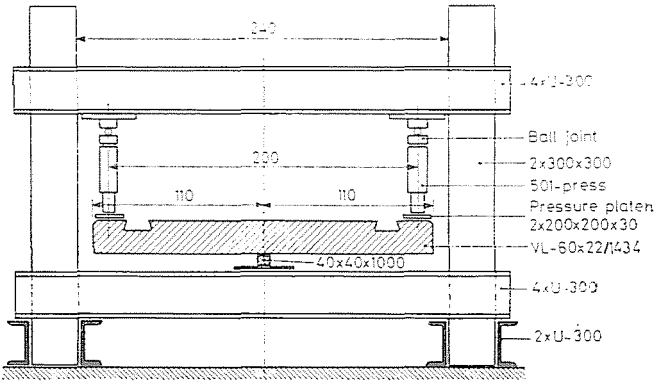

Fig. 26. Loading equipment

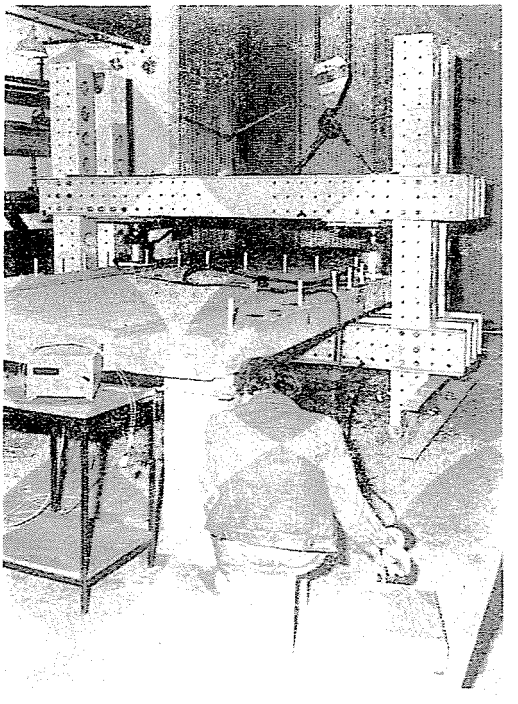

Fig. 27. Equipment for static failure test

surface of the track slab the load distributing upper plates are positioned of $200 \times 200 \times 30$ mm measurements on an interposed load-equalizing gypsum layer. The load was applied by two hydraulic presses of manufacture LUCAS each of them being able to produce maximum 500 kN force. In order to permit undisturbed rotations due to the deformations, spherical hinges are arranged.

In the course of the test investigations the following values have been measured:

a) *Loading force in kN by each press*

Since the matter in question was a static test, the force values have been read at every step of load after the developing process of the decisive majority of the deformations. The evolvement of the deformations needed about 20 to 25 minutes.

In the following, each flight of loading is designated by the magnitude of the force applied by one of the presses expressed in kNs.

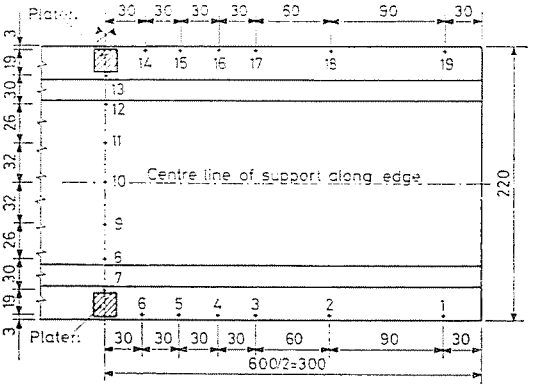

Fig. 28. Arrangement of the measuring points — 1st load

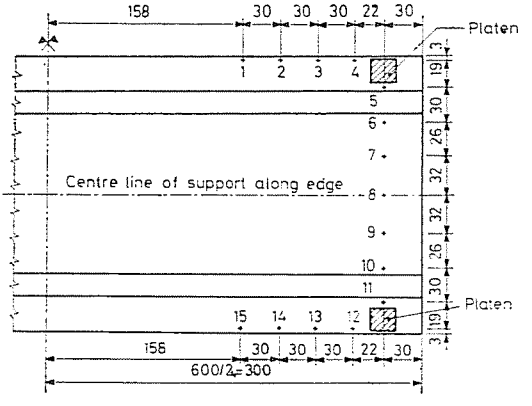

Fig. 29. Arrangement of the measuring points — 2nd load

b) *Deformations of the track slab taking place under the effect of the load*

On the top surface of the track slab strain gauges have been glued at the points as shown in Figs 28 and 29. The vertical displacements of the points of measurements have been measured with the aid of an automatic level type Ni B 1. The exactitude of the measurements may be estimated at ± 0.05 mm.

The ultimate strength tests have been carried out on two track slabs recovered from the track.

3.2.2 *The result of the test*

3.2.2.1 *Test on track slab No. 1*

a) *First loading*

The track slab No. 1 has been examined first at the *centre cross section*. The load pattern and the places of the points of measurements are to be seen in Fig. 28. The load has been applied in flight-to-flight way, and increased up to 110 kN. After reaching the maximum load 110 kN, the load has been eased down to zero. For each step of load deflections have been measured at 19 points.

In order to better visualize the process of testing, the measurement results have been plotted on a graph. In Fig. 30 the transversal deformations of the loaded track slab are to be seen during the application of load directed upwards.

During the application of load to the centre cross section of the track slab No. 1 and augmenting up to 110 kN, *absolutely no changes could be detected* on the track slab including cracks. Also the residual deformations might be considered insignificant.

b) *Second load*

After the load at the centre cross section loading has been applied at the end of the track slab No. 1. The arrangement of the load and the measuring

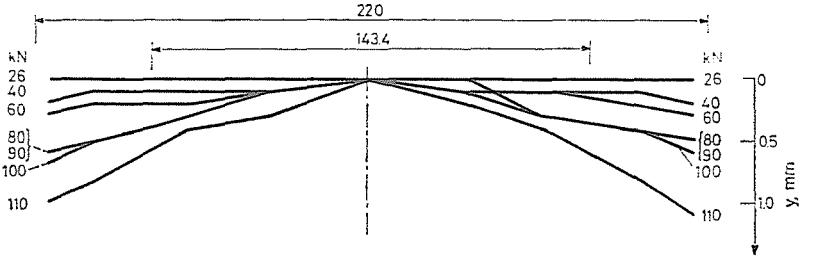

Fig. 30. Deformations of the loaded cross section of the track slab at the different load steps, in case of half load

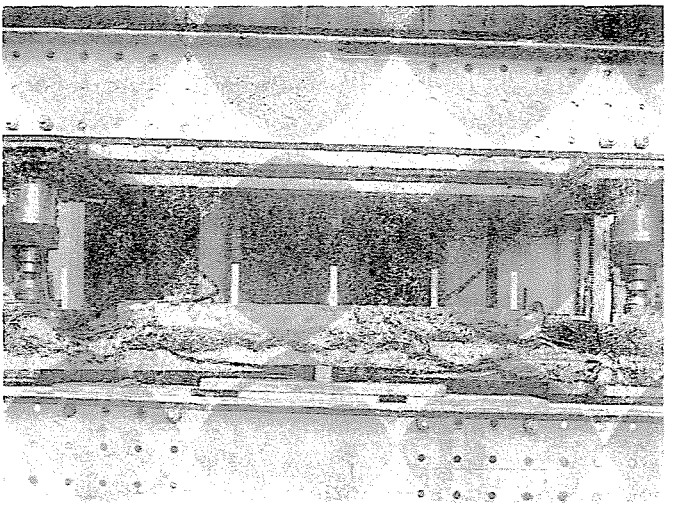

Fig. 31. Failure of the track slab at 130 kN

points is represented in Fig. 29. The load has been augmented in flight-to-flight up to the failure of the track slab.

During loading, at the *step of load* 90 kN *micro cracks* presented themselves along the longitudinal axis of the track slab which, with the augmentation of the load rapidly propagated.

At the *load step 110 kN cracks of nearly 45 degrees* came into being but whose width did not grow any more significantly.

At the *load step 130 kN breaking down* of the bottom part of the track slab took place originating at the corner of the left-hand side rail channel and at the same time, the laminar *separation* of the slab at its centre segment (Fig. 31).

3.2.2.2 *Testing of the track slab No. 2*

The track slab No. 2 has been loaded at its centre cross section up to the failure. The arrangement of loading and the places of the points of measurement are as is shown in Fig. 28. The load has been augmented in the way described above, however, to eliminate initial uncertainties, here also the condition associated with the load 10 kN has been considered as zero point.

In augmenting the load, at the *load step 140 kN*, at the centre of the track slab *longitudinal* micro cracks occurred which thereafter propagated towards the edges of the track slab at a direction approximately 45 degree in such a way that they reached the longitudinal edge of the panel at the one third of its length.

At the load flight 180 kN the central longitudinal cracks clearly visible even to the naked eye and, at the same time, separations occurred at the inside edges of the rail channels, at the meeting of the concrete and the steel plate

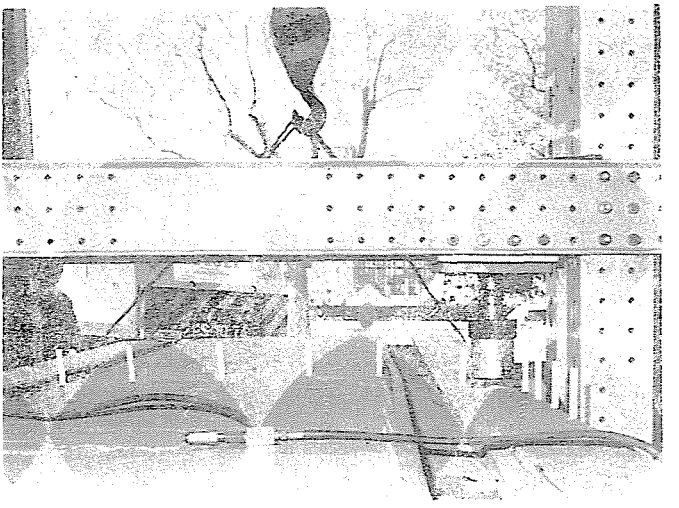

Fig. 32. Failure of the lining of the rail channel

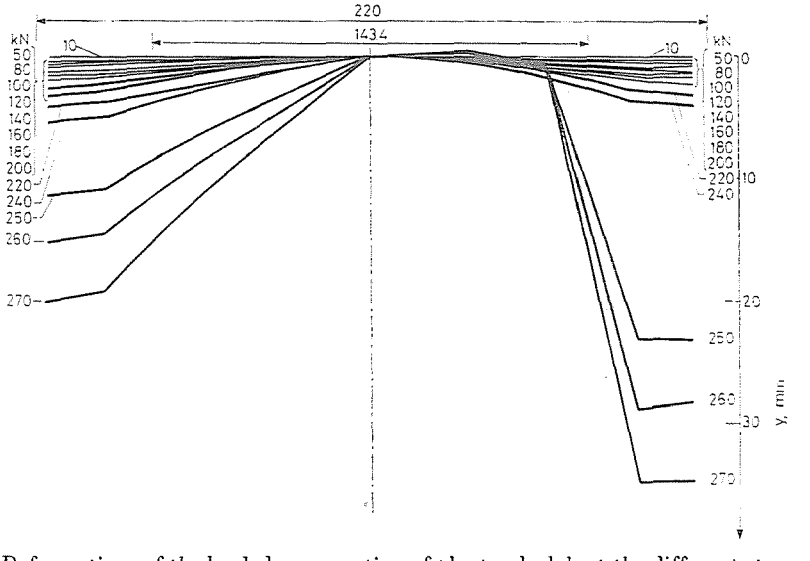

Fig. 33. Deformations of the loaded cross section of the track slab at the different steps of load

and vertical crackings have taken place along the section below the load distributing plates, on the vertical edges of the track slab.

At the *load step 270 kN* the outer edge of the line plate of the left-hand side rail channel became corrugated, wherefore, the *track slab became unserviceable to resist any force thereafter* (Fig. 32).

One of the deformation diagrams of the track slabs No. 2 is demonstrated as an example in Fig. 33.

By way of summing up, it is to be stated that the ultimate load obtained in case of an extraordinarily unfavourable support was in every case higher than the design load of the road vehicle serving for basis to the dimensioning. The tests verified that the track slabs having been in service for years could resist the loading effects of the road vehicles within a high safety standard without any damages.

3.3 Examination of the surface roughness of the r.c. track slab

From the point of view of the safety of the road vehicle traffic the surface roughness of the r.c. track slabs is of high significance.

The measurement of the surface roughness has been carried out with the aid of the friction-measuring balance developed in England (SRT) taking also the prescriptions of the standard of the Hungarian Ministry of Transport and Communication (KPMSZ-Ut 9—76) into account.

To the measurements new track slabs stored waiting for being laid in, and those recovered from the track were used. Selecting both from the new slabs types VL-60 and VL-15, and from the used ones type VL-60 three slabs from

Table 10

SRT-values of surface roughness of reinforced concrete slabs measured

No. of slabs	No. of the measurements	Type of r.c. track slabs					
		New VL-60		New VL-15		Used VL-60	
		in axis	on the verge	in axis	on the verge	in axis	on the verge
Slab No. 1	1	85	81	53	52	56	53
	2	85	82	53	53	55	53
	3	84	82	53	54	56	52
	$\bar{x}_1$	84.67	81.67	53.00	53.00	55.67	52.67
Slab No. 2	1	82	88	44	41	62	57
	2	82	88	45	43	60	58
	3	82	88	45	43	60	58
	$\bar{x}_2$	82.00	88.00	44.67	42.33	60.67	57.67
Slab No. 3	1	72	60	36	57	55	51
	2	72	61	37	57	53	50
	3	72	61	38	56	53	50
	x_3	72.00	60.67	37.00	56.67	53.67	50.33
Final roughness values	$\Sigma\bar{x}$	79.56	76.78	44.89	50.67	56.67	53.56
	$\Sigma\Sigma\bar{x}$	78.17		47.78		55.12	
	S	±9.49		±7.17		±3.55	

Notation: Σx = average values of the results of measurements carried out on slabs 1 to 3 (at their centre line and edges); $\Sigma\Sigma x$ = average values of the results of measurements carried out on slabs 1 to 3; S = scatter of the measurement results

Table 11

Sign of the traffic situation	General description of the traffic situation	SRT value suggested
A	Before stop lines and zebra-crossings, in curves of radii shorter than 150 m, in junctions, crossings and road sections of larger slope than 6 per cent	65
B	On rapid transit roads, on national and town main roads	55
C	At other places	45

each types, the friction resistance of the wetted concrete surface has been measured at two points on each of the slabs by using the measuring instrument mentioned according to the relevant regulations.

The measurement results read have been corrected by taking the temperature of the slab into account according to the pertinent prescriptions.

The measurement results suitable to the evaluation are contained in Table 10 while in Table 11 the values of the relevant Hungarian standard prescriptions are presented.

4. Examination of the assembled finished track structure

4.1 Stability of the track structure against buckling

4.1.1 *Stability of the track slabs*

In carrying out the research investigations, the stability of the track constructed by making use of the r.c. track slabs, against deflection has been determined with the aid of the calculation method familiar from the basic principles of the track of continuously welded rails.

4.1.1.1 *Stress pattern in the track slabs*

— Change in length caused by the change of temperature in case of unhindered displacement of the track slab:

$$\Delta l = \alpha \cdot l \cdot \Delta t = 5.78 \text{ mm}$$

— The design heat force:

$$P_M = \alpha \cdot E_b \cdot A \cdot \Delta t = 4975 \text{ kN}$$

4.1.1.2 *Vertical deflection of tangent track segment*

— The minimum force causing deflection:

$$P_{\min} = 10\,080 \text{ kN}$$

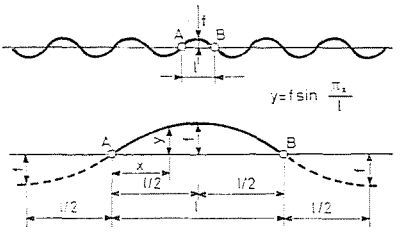

Fig. 34. Initial deficiency in track laying

— Safety against vertical deflection:

$$n = \frac{P_{\min}}{P_M} = 2.03$$

— Critical wavelength of the deflection:

$$l_{kr} = 29.05 \text{ m}$$

4.1.1.3 *Horizontal deflection of tangent track segment*

— In case of an initial defect in the alignment to be seen in Fig. 34, the minimum deflecting force will be:

$$P_{\min} = 67\,637 \text{ kN}$$

— The safety against the horizontal deflection is:

$$n = \frac{P_{\min}}{P_M} = 13.59$$

4.1.1.4 *Horizontal deflection of a curved track*

— The minimum force causing the displacement of a curvilinear track in case of the minimum radius $R = 40$ m permitted to be applied, is:

$$P_{\min} = 20\,400 \text{ kN}$$

— The safety against the horizontal deflection is, in a track lying in a curve of a radius $R = 40$ m:

$$n = \frac{P_{\min}}{P_M} = 4.10$$

4.1.1.5 *Summary*

From that said above may unequivocally be pointed out that the track laid with r.c. slabs in stable both against the vertical as horizontal deflections. Merely the total deflection of the curvilinear segments not yet built into the road pavement may be somewhat dangerous, namely, the friction force taking

place on the bottom surface of the slabs does not represent an appropriate lateral resistance. However, after the construction of the road pavement adjoining to the slab, it will get such a lateral support that the required safety against deflection will be completely assured.

Therefore either *expansion joints* should be applied at the commencement and termination of the curves, or the track slabs should only be closed to each other after the rebuilding the contiguous road pavement strip.

In the latter case, the road pavement should be constructed by the strict observance of the road building technique, to assure the appropriate lateral support to the track. Construction of a pavement from big blocks should be avoided, because according to the experiences for lack of the cooperation they will vertically displace and come out of the plane of the slabs, wherefore, the value of the lateral support will diminish.

4.1.2 *Stableness of the block rail*

The Department for Railway Construction carried out theoretical and experimental research investigations for the determination of the stableness of the rail of the block-rail track structure against deflection. Carrying out the series of tests was motivated by an earlier, vertical deflection which took place during track laying at a hot summer temperature on the network of the Budapest tramway (Fig. 35).

4.1.2.1 *Stability examination of the block rail against deflection by making use of field tests*

In the course of the tests first the vertical stableness of a 12 m long (the length of two track slabs) block-rail against deflection has been examined, the axial compressive force has been produced by heating the rail (Fig. 36). In the second series of the tests a rail 6 m long (equal to the length of a track slab) has been tested, the compressive force parallel to the rail axis has been applied by hydraulic presses (Fig. 37).

The determination of the compressive force has been carried out in case of heating the rail with the aid of thermometers placed in the rail head, and in case of applying the test load by hydraulic presses, by reading off the values shown by the precision manometer which was integrated in the oil pump.

Let us see Fig. 38, as an example, in which the vertical displacements are demonstrated observed at cross sections spaced 1 m from each other of the 6 m long rail. After augmenting the load (see figure) up to 1570 kN, whereat, the rail together with the tensioning rubber strip, associated with a strong sound effect, has been burst out of the rail channel of the slab. The form of the deflected rail which is covered by the clamping jaws, may well be discriminated with the aid of the measuring lath (Figs 39 and 40).

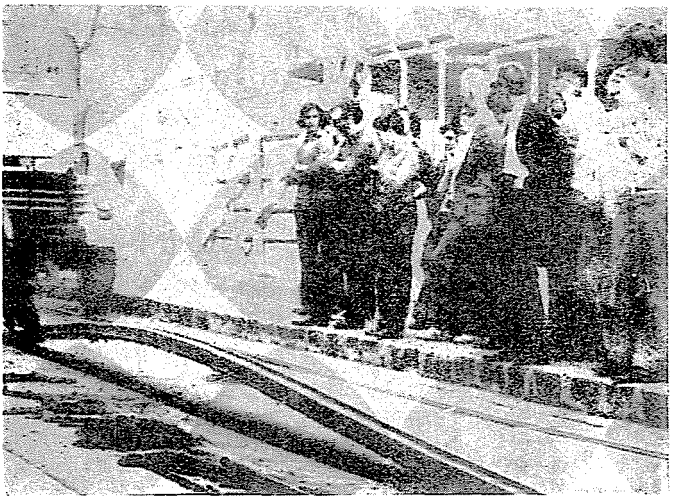

Fig. 35. Vertical rail deflection in the course of track construction

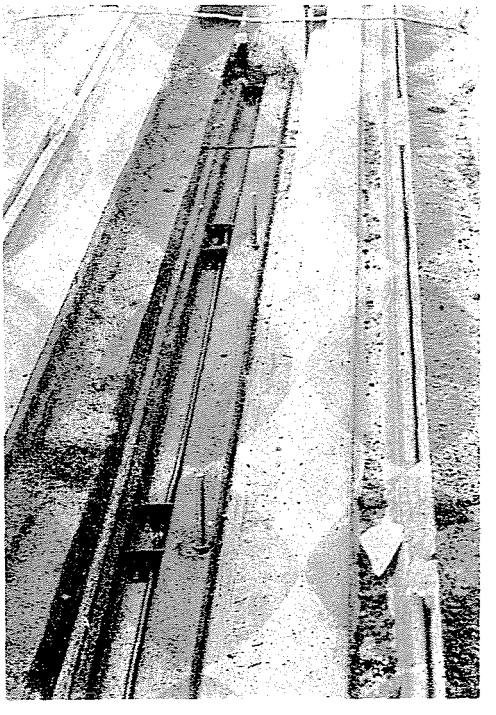

Fig. 36. Producing compressive force in the rail by heating in the direction of its longitudinal centre line

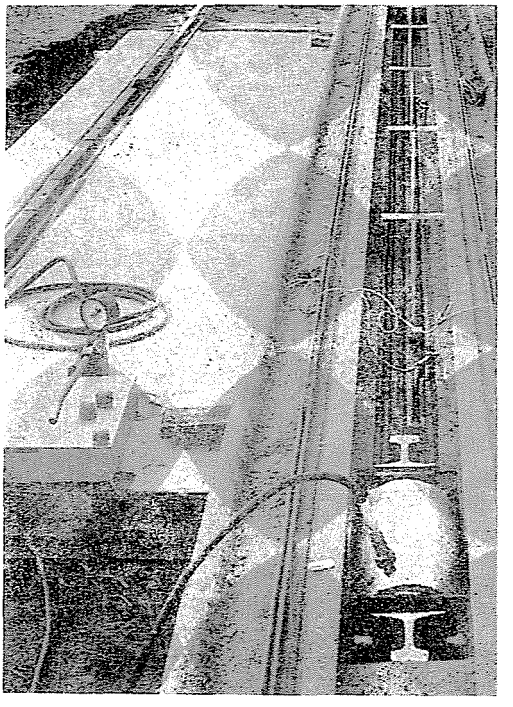

Fig. 37. Producing compressive force in the rail with the aid of hydraulic press in longitudinal direction

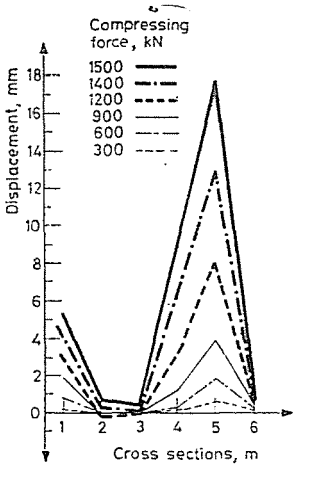

Fig. 38. Vertical deflection of a 6 m long rail

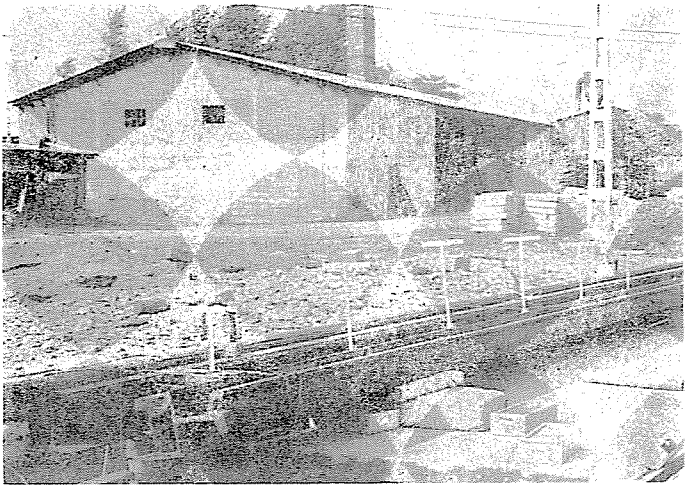

Fig. 39. Deflection of rail in testing

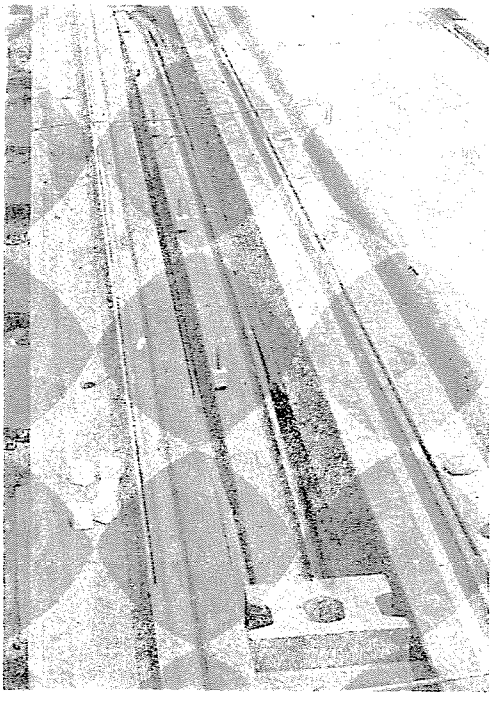

Fig. 40. Deflection of rail during testing

4.1.2.2 *Tests to draw out the rails*

The resistance to vertical drawing out of the rails has been determined by extraction tests. The tests have been conducted with several rail sections of different lengths (100, 200 and 400 mm), and from the results obtained, the extraction diagram of the unit length of the continuous rail has plotted by extrapolation. In Fig. 41 the extraction test of the rail segment of 200 mm length is to be seen. Tests have been performed with both of rails fixed with elastic strips as prescribed, and unfixed rail segments. The values of the spring characteristics obtained have been utilized in the theoretical calculations.

4.1.2.3 *Stability calculations of the block rail*

From the point of view of the vertical deflection the rail can be theoretically considered to be an elastically embedded and, in the examined region of deformation, an unrestictedly elastic compressed bar. The deflecting force of this structure is defined

— by the bending stiffness EI of the elastic bar and
— by the characteristic curve of the elastic bedding.

With detailed calculations has been examined whether the change of the basic parameters — first-those characterizing the elasticity of bedding — what

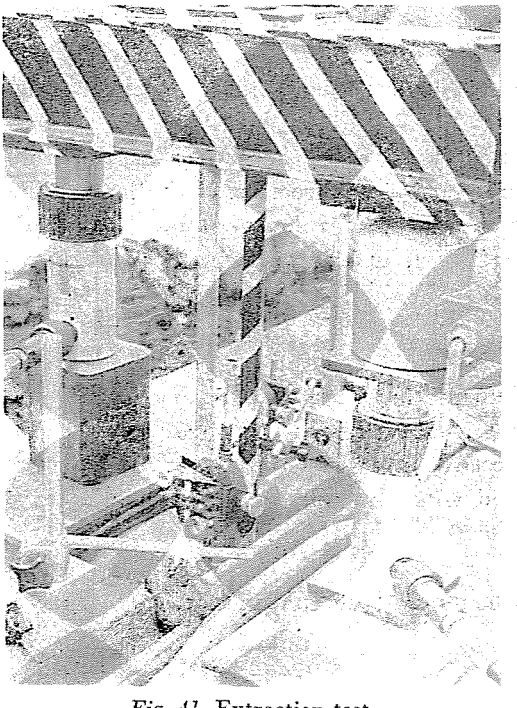

Fig. 41. Extraction test

an effect exercise upon the deflecting force of the rail, i.e. what requirements should the characteristic curve of bedding and the other characteristics of the track meet to make the track sufficiently safe against deflection.

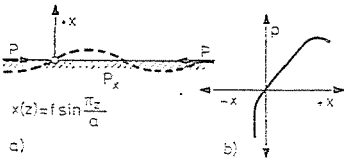

Fig. 42. Model of the calculation

The model of the calculation problem is to be seen in Fig. 42. The solution has been found by using the familiar method of the stability theory. The three basic conditions of the calculation are as follows:

1. The bending stiffness of the rail EI is along the longitudinal axis of the rail constant and, the curvature d^2x/dz^2 does not cause anywhere plastic deformation.

2. The characteristic curve of the bedding can be described with some resistance p

$$p = p(x)$$

is only the function of the deflection x but is not the function of the longitudinal coordinate z.

3. It is assumed that during the deflection, the cross sections of the rail can displace unhindered in the direction of the longitudinal axis.

The elasticity potential π of the system investigated — in case of a given compression force P — is in any static, i.e. equilibrium condition constant:

$$\pi = E_a + E_h = \text{constant}$$

wherein: E_a — deformation energy of system
E_h — potential energy of force system.

Assuming the two potential equilibrium conditions, the elastic potential difference associated with the two conditions can be expressed as follows:

$$\Delta\pi = \Delta E_a + \Delta E_h = 0.$$

It can easily be pointed out that in steady equilibrium state the condition

$$\Delta\pi = \text{min}\,!$$

is to be fulfilled.

Disregarding the detailed calculations here only the equation of the elastic potential is presented:

$$\Delta\pi = \frac{\pi^4}{4} EI \frac{f^2}{a^3} + \frac{2}{4} \frac{p_{\max}}{x_m} f^2 a - \frac{2}{9\pi} \frac{p_{\max}}{x_m^2} f^3 a - \frac{\pi^2}{4} P \frac{f^2}{a} - \frac{\pi^2}{2} P \frac{ff_0}{a}$$

Two free parameters are in the equation, the versine f and the upper wave length a. From two equations of the equilibrium conditions the relationship

$$P = P(f, a)$$

has been determined. Prior to the numerical solution in assuming the starting data, the scatter of the spring characteristic causes difficulties (due to the inaccuracy of the measurements of the structural elements, and to their variable material quality) as well as the effect of aging of the rubber parts.

To consider the scatter of the spring characteristics valid at the time of the track laying five values significantly differing from each other have been assumed between the limiting values $p = 5$ to $p = 60$ kg/cm. In order to study the effect of aging it has been assumed that as a result of this process the displacement x_m will be augmented meanwhile with the reduction of the specific force $p_{\max}$ in such a way that the production of the two values remains constant:

$$K = p_{\max} \cdot x \left[\frac{\text{kg}}{\text{cm}} \cdot \text{cm} \right].$$

The detailed calculations worked out for 15 problems, are to be found in *Report 9*. By way of summary two figures are here presented:

In Fig. 43, the relationship between the deflecting force $P_{\max}$ and the coefficients $p_{\max}$ and K is to be seen. From the figure the maximum value of the specific spring constant $p_{\max}$ in the case of $t = 60$ °C, for different specific spring work K may be read. On this basis the limiting curve shown in Fig. 44 can be plotted which prescribes the values of $p_{\max}$ and x_m, which are needed to be reached to assure the safety against deflection. In the figure, the curve segment associated with the values higher than $x_m = 20$ mm is designated by dashed line, because, due to the discontinuance of the powerful tensioning effect of the rubber strip, cannot practically be taken into account.

The block-rail track laid strictly *according to the relevant prescriptions with the rubber strip* has, as the calculations made by the University Department for Railway Construction show, a proper safety against deflection in case where

— the initial curvature, i.e. the versine measured on a cord length 3000 mm does not surpass the 4 mm.

In case of a rail fastening *without rubber strip* can be established that

— the deflection might take place depending on the initial eccentricity already in case of a temperature difference $\Delta t = 15$ to 20 °C and

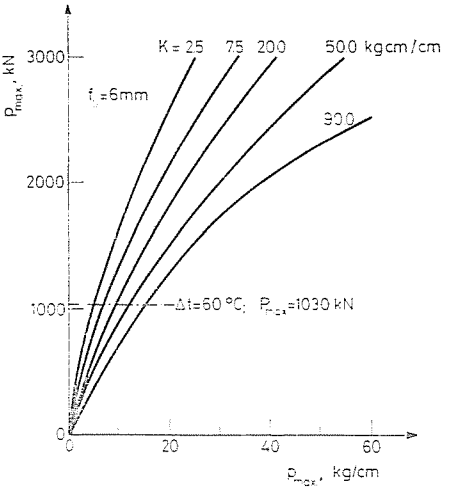

Fig. 43. Relationships between P_{max}, p_{max} and K

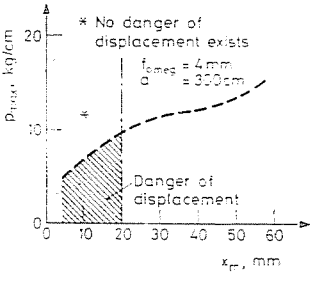

Fig. 44. The limiting curve calculated

— the deflection is entirely elastic buckling, i.e. the initial state will be re-established with the cooling of the rail without any damage of the rail.

4.1.2.4 *Estimation of the tests and the calculations*

From the theoretical calculations and test investigations could be established that in case where the closing weld of the block rails and the impression of the rubber strip to fix the rails takes place above +5 °C rail temperature in a regular way, a vertical rail deflection does not occur either at the highest temperature which might occur. This significant statement is conditioned by the elastic, regular behaviour of the rubber strips.

In case of the block rail laid without rubber strips, for example, during track laying, before its completion, in dependence upon the initial eccentricity, even at an augmentation of the rail temperature to Δt = 15 to 20 °C, vertical

rail deflection might occur. Such an event took place at the instance demonstrated in Fig. 35.

As a result of the investigation, with a view to augment the track stableness, the following has been suggested:

— During the impression of the fastening rubber strip, its elongation should be reduced to the minimum possible.
— At the adjoining of the r.c. track slabs the stepped joints taking place in consequence of the uneven support — also in the interest of stability preservation — should be eliminated, i.e. their development should be prevented.
— Grading up the quality of the r.c. track slabs, mainly the elimination of the torsional deformation and the preservation of an appropriate running surface also fosters the augmentation of the stableness.
— The joints at meeting of the r.c. track slabs and the road pavement are to be maintaned with care; pumping up the the soil should be prevented.

4.2 Examination of the slip of the track structure

It has been examined whether the r.c. track slab structure with block rails laid in a road pavement lying on a steep gradient is not subjected to the danger of slipping down along the slope.

The *active forces which could cause the slippage* are as follows:

a. Downslope sliding force calculated from the net weight of the r.c. slab (on 60% slope) ..... $F_1 = 3$ kN

b. Downslope sliding force calculated from the gross weight of the vehicle (weight of the vehicle on 60% slope) ..... $F_2 = 12$ kN

c. Braking force of downslope direction of road vehicle . $F_3 = 140$ kN

Active sliding forces altogether ..... $F = 155$ *kN*

The braking force of the tram vehicle in the downslope direction (calculated from the braking deceleration and the data of the vehicle $F_4 \leq 90$ kN) is not to be taken into account since the track structure is assembled with jointless bars wich cannot be displaced along the longitudinal direction.

Thus, it is to be seen that besides the almost negligible dead weight of the track structure prevailingly the braking effect of the heavy lorries transmits to the slabs a significant downslope sliding force parallel to the track centre-line in comparison with which the steepness of the slope is a negligible value.

The active sliding forces are resisted by the frictional force arising

— on the bottom support surface of the track slab,
— between the lateral side surface of the track slab and the road pavement,
— between the tensioning rubber strip and the railseat channel.

The reaction force caused by the jamming up of the track slabs must not be taken into account since this phenomenon cannot be permitted to develop from the point of view of the stableness of the track slabs.

The resistance to the slip of the track slabs has been determined with the aid of *field tests* by which the following occurrences have been investigated:

1) In case of an r.c. track slab put upon an asphalt bedding layer *without rails:*

a. unloaded slab, dry bed;

b. slab loaded by two more slabs, dry bed;

c. slab loaded with a lorry of 95 kN gross weight;

d. unloaded slab, wet bed.

2) Slab laid in a *track assembled* to the relevant prescription

The test set-up is shown in Figs 45, 46 and 47. Figure 48 represents, as an example, a force-displacement diagram plotted during carrying out the tests. The diagram can be divided, as demonstrated in the figure, into three regions:

a. Elastic region between the forces 0 and P_A,

b. Elastic-plastic region between the forces P_A and P_F,

c. Plastic region above the force P_F.

Up to the force P_A no residual displacement occurs but, at the loading force P_F already a residual displacement may be observed. Thus, in the elastic

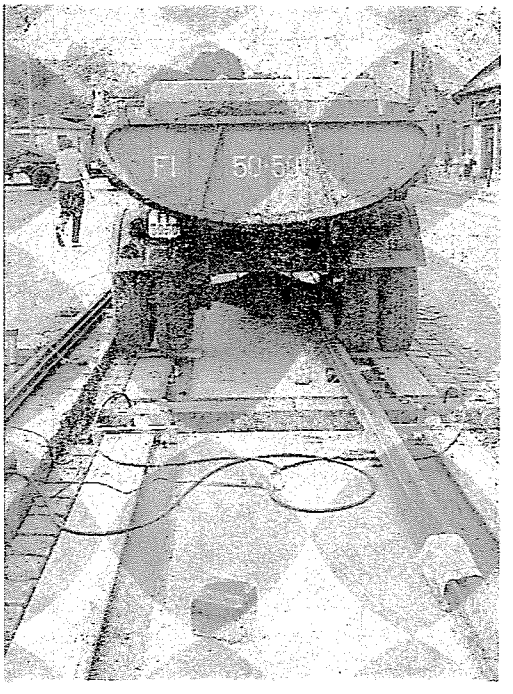

Fig. 45. Sliding test on the track slab

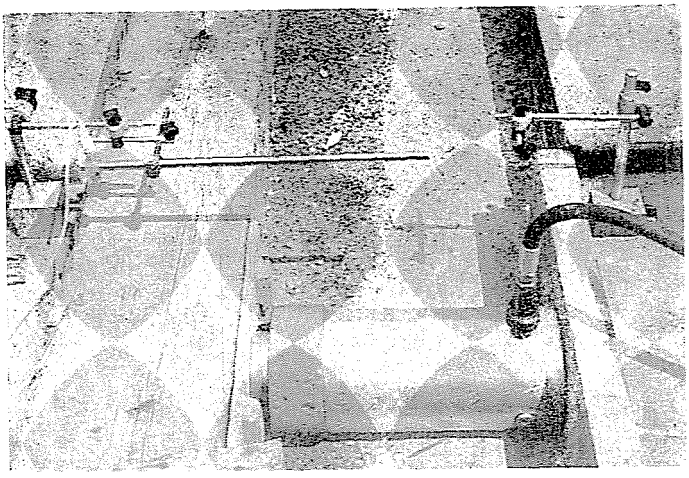

Fig. 46. Shift test on the track slab with hydraulic press

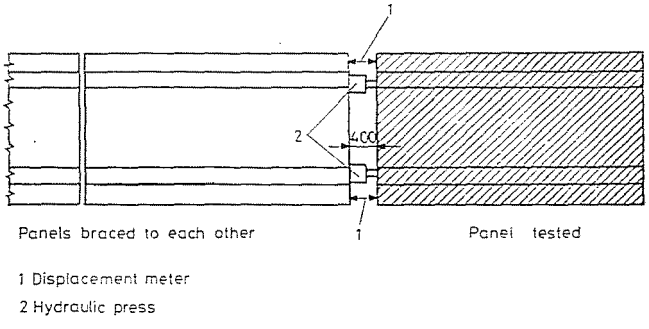

Fig. 47. The test setup

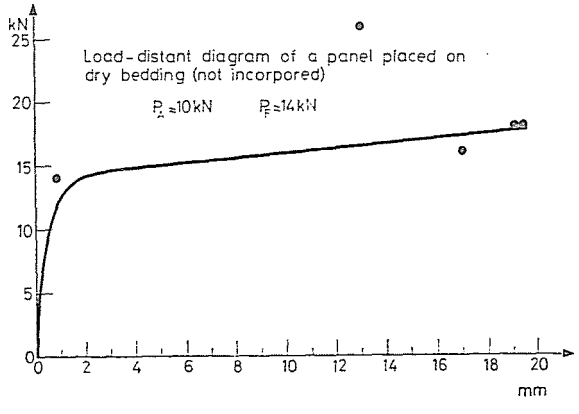

Fig. 48. Force-displacement diagram of the track slab laid on dry bedding

Table 12

Application mode and load conditions of the r.c. slab	Shear force [kN]	
	P_A	P_B
Non-incorporated, unloaded slab, dry bedding	10	14
Non-incorporated slab loaded with two slabs, dry bed	25	50
Non-incorporated slab, loaded with a lorry of 95 kN, dry bed	15	27
Non-incorporated, unloaded slab, dry bed	8	12
Slab mounted, laid in the track	27	120

region no residual displacement develops, in the elastic-plastic region the increasing displacement is associated with an increasing force, while in the plastic region the increasing slab displacement is associated with an approximately constant force.

The values of the forces P_A and P_F obtained from the test results are indicated in Table 12.

From the experimental investigations the following results can be concluded:

— To the continuous displacement of the r.c. track slabs laid according to the prescription into the track an active sliding force 120 kN is needed.

— In dependence on the condition of the track longitudinal forces even as low as 8—27 kN can cause residuary deplacement.

— Disadvantageously repeated road-vehicle loading and repeatedly braking heavy vehicles can induce movements and jamming up of the slabs. The actual value of the maximum sliding force 155 kN caused by the heavy lorry is somewhat reduced by the fact that, in general, not all of the four wheels are braked on the very same slab.

— The slab displacements experienced during the series of the tests have taken place firstly in consequence of the creep of the asphalt cover on the bedding.

— The longitudinal slope of the track does not influence significantly the slip of the r.c. track slabs.

— In view of increasing the stableness of the track slab it would be advantageous to apply friction-increasing or anchoring structural elements.

4.3 Laboratory tests on the rail fastening

The investigation has been extended to the laboratory fatigue tests of the *block-rail fastening* in the track slab structure by applying *rubber fastening strip*.

In the course of the test series, the block rail fastened to the track slab has been subjected to repeated flight-to-flight loading by continuous measurement of the vertical and horizontal displacements of the block rail which charac-

terize the state of the fastening equipment. Meanwhile the change of state and the behaviour under the loading of the track slab, the rubber pad supporting the rail and the fastening rubber strip has continuously been recorded.

4.3.1 *Methods and instruments of the fatigue tests and their performance*

To the test of the rail fastening equipments it is the *scissors vibration* which is the most appropriate to realize the closest simulation of the actual loading. This testing method is well-known from the literature on the subject its several versions differing only in details are familiar (ORE, OSZZSD, etc.).

The *Department of Railway Construction of the Technical University Budapest* has been worked out a similar investigation method which has successfully been applied for several years for a number of series of tests using *heavier loading than other familiar endurance tests.* By this method the tests are carried out by applying five sine-form loads of gradually augmented weigth; the frequency is 5 Hz.

The *load stages* are as follows: Table 13

At each flight of load prior to the endurance test *static up and down load* have been carried out from zero to the maximum force of the given load flight.

Table 13

Load stage	Number of repetition of the load	Loading force
I	to $1 \cdot 10^6$	$F = 5$ to 50 kN
II	to $2 \cdot 10^6$	$F = 5$ to 75 kN
III	to $3 \cdot 10^6$	$F = 5$ to 100 kN
IV	to $4 \cdot 10^6$	$F = 5$ to 150 kN
V	to $5 \cdot 10^6$	$F = 5$ to 200 kN

By the tests the *vertical displacement of both block rails* compared to the track slab and the *change in the track guage* have been determined both under the effect of the static and dynamic loads.

The arrangement of the test is clearly to be seen in Fig. 49. In examining the track slabs of large dimensions the anchorage of the loading frame is realized by the *stressing bed* of the laboratory.

The results of the endurance tests can be summarized as follows:

a) *Vertical rail displacements*

— In the case of both of the track slabs of large and smaller measurements, the vertical displacements of the block rails are of values between 0.1 to 2 mm which, even in case of an axle load 200 kN is permissible, although this one is significantly higher than the real one.

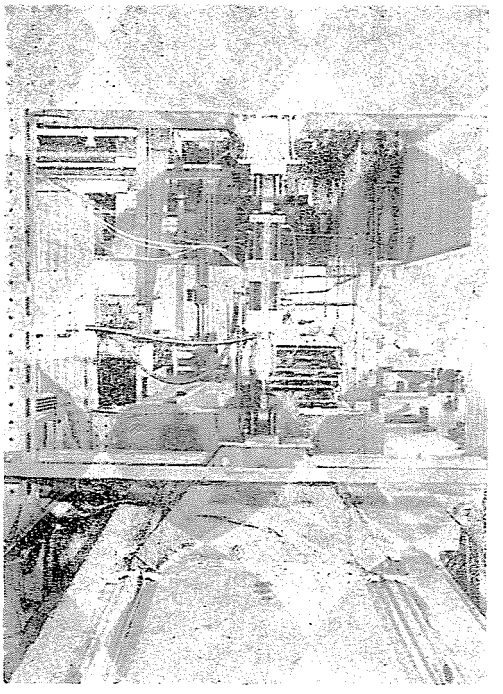

Fig. 49. Fatigue test equipment with scissors vibration

— In the course of the repeated load the value of the permissible vertical rail displacements tends to somewhat decrease rather than increase, the rail fastening so to say "hardens".

b) *Horizontal rail displacements*

— The length of the the rails mounted into the track slabs significantly affects the magnitudes of the horizontal movements and turning off of the rail. The longer the block rail, the less are the movements.
— The values measured are otherwise at the higher load flights also permissible.
— The change in the track gauge hardly reaches the 10 mm, and in reality only the half of it, since differing from the test arrangement, at the same time only one wheel of a wheel set transmits lateral force to the rail.

c) Pulsation of the rail fastening equipment of track slabs of minor measurements showed that applying short rubber fastening strips is not advantageous because they easily contract under the effect of the lateral forces.

The endurance tests pointed out that the rail fastenings of the *r.c. track slabs with block rails resist the repeated loadings*, even in case of wheel loadings higher than the reality, their *destruction is not to be afraid of.*

4.3.2 *Measurement of the resistance to the longitudinal displacement of the rail fastening*

The block rails of the track slab of minor measurements prepared to the endurance test *have been slightly pushed out of the slab*, as is to be seen in Fig. 50.

The force-displacement diagrams plotted pointed out that the resistance of the rail fastening to longitudinal displacement is *satisfying*. In case of a rail failure the development of a significant dangerous gap is not to be reckoned

Fig. 50. Test on pushing out the rail

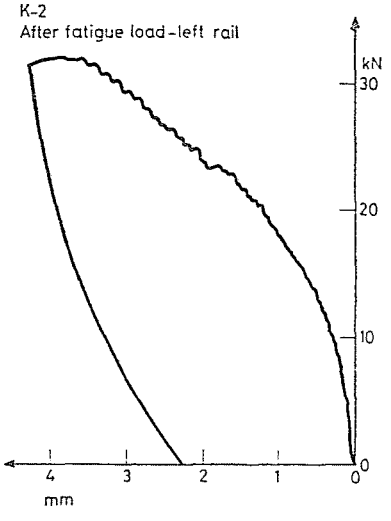

Fig. 51. Diagram of longitudinal pushing resistance

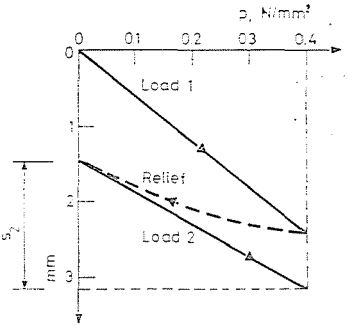

Fig. 52. Load diagram

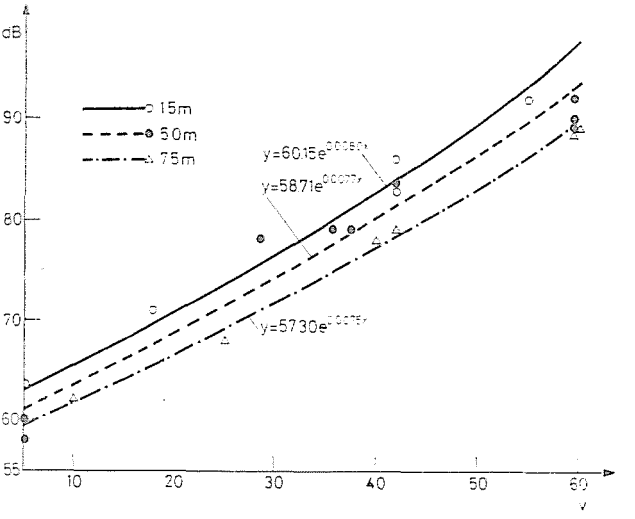

Fig. 53. Noise measurement diagram

with; the rubber elements, under the effect of the repeated loading will slightly stiffen.

4.4 Examination of the impression of the rubber strip

The test series conducted on the rubber strip intended to examine the rate of elongation in the course of its mounting into the track slab.

The tests have been carried out with the aid of a self-propelled rubber impression vehicle transformed to this purpose from a tamper type "Buda". The first series have been performed with different quickness of impression, however, the rubber band has been destructed at the stage of quickness 0.46

m/s. With the second test series the intermittent or partial strip-impression method has been tried, whereby at the first run of the machine the rubber strip has only been impressed to the level of the running face and at the second run down to its final position.

A significant elongation of the rubber strip, such as 30 to 45 per cent, during the process of impression could be considered as disadvantageous. The stuff pressed out of the cross section does not come back any more because neither of the strips can be unloaded at its full length at the same time.

By applying the intermittent method of the impression of the rubber strips, their elongation could significantly be reduced; the "softening" of the rail fastening by preserving its stableness against deflection, would be serviceable to the large panel system.

4.5 Foundation problems of the track structure

4.5.1 *Deficiencies of the current design*

The experience made during twelve year's operation of the r.c. slab track system with block rails as well as the investigations conducted by the University Department for Railway Construction unequivocally emphasize the significant function which is to be served by the founding and bedding layers supporting the track slabs, in connection with the quality, stableness, elastic resistance to loads, etc.

The general leading principle of the construction of the track structure is that the quality, specific load bearing capacity of each of the layers of the track structure and the values of the coefficients of the layer-equivalent "e" expressing the above characteristics, gradually increase from underneath upwards. The r.c. track slab structure does not satisfy this principle because the concrete slab is directly supported by a loose bedding layer. Although one does not require a good load bearing capacity from that layer, however, it is an engineering contradiction that between two compact layers which effectively participate in load bearing, a loose layer is to be found. In this depth such stresses are induced which lead to the deformation of this layer, especially in case where its density is uneven.

The technique of track laying prescribes, independently of the traffic load, uniform thickness measurements to the foundation layers to be constructed. This prescription results in some cases in overdimensioning, however, in the majority of cases in a poorer construction. At all events, the dimensioning of the substructure becomes necessary both to the road and the tramway traffic.

Also the field measurements presented below point out the extraordinarily wide scatter of the quality of the construction work.

Table 14

Signs of the system of bedding	Denomination of the system of bedding	Denomination of the track structure layers	Thickness of the structural layers (cm)
I	Bituminous concrete bed on concrete slab	— track slab	18
		— non-compacted bituminous concrete AB-5	2—3
		— non-compacted bituminous concrete AB-20	6—8
		— monolithic concrete B 210	15—20
II	Bituminous concrete bed on compacted crushed stone bedding	— track slab	18
		— non-compacted bituminous concrete AB-5	2—3
		— compacted bituminous concrete AB-20	6—8
		— crushed stone bed. Z.35/55	20—30
III	Injected goute bedding	— track slab	18
		— injection grout	2—4
		— compacted bituminous concrete AB-20	6—8
		— monolithic concrete B 280	15—20
IV	Non-compacted asphalt concrete structure without bedding layer	— track slab	18
		— where needed rubber-bituminous grouting	—
		— non-compacted bituminous concrete AB-20	6—8
		— monolithic concrete B-280	15—20
V (Not realized on site)	Sand bed with emulsive bitumen	— track slab	18
		— sand bedding	1.5—2.0
		— compacted bituminous concrete AB-20	6—8
		— crushed stone bedding Z.35/55 or	20—30
		— monolithic concrete B-280	15—20

Table 15

Place of measurement	Centre of the panel	Corner of the panel	Foundation	Year of construction
Irinyi J. street	44	24	concrete	1980
Alkotás street, No. II.*	200	100	concrete	1976
Alkotás street, No. III.	14	49	crushed stone	1976
Május 1 road	27	26	concrete	1975
Mezõ I. road	16	35	crushed stone	1978

* Effect of a construction defect revealed posteriorly

4.5.2 *Performing and estimating of the tests*

To the purpose of the tests the realization of five types of designs has been suggested to the tramway diretion, however, the design of bitumen-emulsive sand bedding indicated in the last line of Table 14 has not been realized.

From each of the foundation designs a segment of 18 to 30 m length (3 to 5 track slabs) has been laid in the street "Török Flóris". The measurements have always been performed on the centre slabs, the 1st, 6th and 10th week after putting the track newly laid into service. Until the last measurement one could reckon with a total loading of 1 200 000 gross tons which has been rolled over on the slabs in question.

The investigations have been extended to the following.

4.5.2.1. *Examination of the elasticity of the foundation methods*

The objective assumed was the determination of the subgrade coefficient under the rail which took place with the aid of stresses determined on the basis of Hooke's law, obtained by using strain gauges

$$C = \frac{4EJ}{s}\left[\frac{Z}{4 \cdot \sigma \cdot K_t}\right]^4 [\mathrm{N/mm^3}]$$

wherein s — width of substituting longitudinal beam, mm
σ — stress measured at rail-foot middle, $\mathrm{N/mm^2}$
K_t — resistance coefficient of rail with respect to rail foot, $\mathrm{mm^3}$

For the measurements carried out under a motor coach type 1500 three stages of speed have been used, the results obtained have been processed by computer.

The significant scatter of the load bearing capacities of the beddings in plan catches immediately one's eye.

It is interesting that the results in question were very similar to those obtained by the measurements of the same nature carried out by the Technical University of Prague.

On the basis of estimating the measurement results, the following conclusions can be made:

— On the test track the compaction of the subgrade can be observed.
— The scatter of the values of the subgrade coefficient reduces in time which is connected with the phenomenon of taking up the settled final position.
— The track structure is the stiffest at the 1st and 2nd test section. The comparatively high elasticity of section 3 is presumably only apperent, it may be the consequence of the support on points. The strain gauges of slabs underhollowed showed stresses after suppression of the load.

— The change in the scatter of the coefficient of subgrade in dependence on the speed of the vehicle or more exactly on its dynamic effect mirrors the uniformity of the track level.

4.5.2.2 *Examination of the vertical stability of the track slabs*

This examination has been carried out by using a precision level instrument Ni-002, with an exactness within one hundredth mm, and determined the residual vertical displacements of the slabs laid in the track, between two points of measurement. Since the test sections have been constructed on same kind of soil, wherefore, the difference measured between the deflections characterizes also the stability of the foundation layers. It can be stated that a *great part of the settling takes place in a short time* in case of a ground of a sufficient load capacity. *The movements of the track sections are, one or two weeks after putting them into service insignificant, and the track can be considered having a good stability. The stability characteristics of test sections I and III are better than those of test sections II and IV, these latter can be classified lower on the basis of their characteristics.*

4.5.2.3 *Examination of the characteristics of the track geometry*

On the three middle track slabs of each test section, i.e. at lengths of 18 m the most significant characteristics of the track geometry have been determined.

The effect of the subgrade quality is mirrorred in the first line by the change in time of the superelevation, one of the three characteristics mentioned above, however, a cant settling of the track also can cause changes in the gauge due to the stronger wear of the rail head. For classifying the subgrade, the mean values and the scatter of the measurements have been established.

The conclusions which can be made on the basis of the data are as follows:

— At all of the test sections the *augmentation of the track gauge* can be observed which is caused by the wear of the rail head.
— From the *scatter* of the gauge measurements one can make conclusion to the quality of *state of the tracks.* Namely in tracks with a lot of level deficiencies the effect of the wear of the rails is varying, wherefore, a larger scatter is to be found of the measured values of the gauge.
— The test sections laying in succession after each other, make up together a length 150—200 m, constructed as a basis for comparison. Even within this short length significant differences could be measured between the values of the *superelevation* of the different track slabs. The changes in the superelevation of the slabs measured at points spaced 1 m, covered practically shorter or longer cant settlings.

— The *scatter of the values of the superlevation* significantly augmented in time due to the uneven density in space of the subgrade.

4.5.3 *Strength calculation of the foundation*

In dimensioning the foundation, besides assigning the characteristic data of the load bearing capacity of each structural part using the table of these data, also the knowledge of the load bearing capacity of the subgrade is needed. During the construction the modulus of the bearing capacity (i.e. the elasticity) E_2 N/mm² can be determined on the finished earthwork from the results of the so called disc measurement.

The process of the measurement and the way of calculation is prescribed by the Hungarian Norm MSZ, 2509.

The disc of 30 cm diameter of the equipment is pressed to the surface of the earthwork by a hydraulic press, applying the back bridge of a lorry as a counterbalance. After reaching the pressure $p = 0.40$ N/mm², the load should be suppressed, thereafter reiterated. To establish the value of the modulus of elasticity the associated values of pressure-displacement of the second load should be taken into account in the way to be seen in Fig. 5. The modulus of elasticity of the lower basement layer is:

$$E_2 = \frac{\pi}{2} \frac{(1 - \mu^2) p \cdot r}{s_2} \text{ [N/mm}^2\text{]}$$

wherein

μ — Poisson's ratio,
p — highest load = 0.40 N/mm²,
r — radius of loading disc = 150 mm,
s_2 — setting after second load(mm).

Value of μ commonly used for soils
— granular soil: $\mu \cong 0.2$
— cohesive soil: $\mu \cong 0.4$

For practical use the following simplified relationship may be applied:

$$E_s \cong \frac{1.5\ p \cdot r}{s_2} = \frac{90}{s_2} \text{ [N/mm}^2\text{]}$$

The modulus of elasticity of the theoretical layer substituting the multi-layer track structure has been established by making use of the procedure worked out by the Hungarian Railway Research Institute.

— Value of the subgrade coefficient:

$$C = \frac{p}{y} = \frac{E_e}{f}$$

wherein:

$$f = \left[\frac{r}{a} \operatorname{arctg} \frac{\sqrt{a}}{r} Z\right]_0^Z \text{ [mm]}$$

and $a = 0.25$

— The modulus of elasticity:

$$E_e = \frac{f}{4 s_0 \sqrt[3]{E_s \cdot I_x}} \left[\frac{Z(1 + t\bar{s})}{y_e}\right]^{4/3} \text{[N/mm}^2\text{]}$$

where:

s_0 — width of rail flange [mm],
E_s — modulus of elasticity of rail [N/mm^2]
I_x — moment of inertia of rail with respect to axis x [mm^4]
Z — wheel load [N]
t — coefficient depending on required probability
$\bar{s}$ — scatter of mean value
y_e — rail deflection permissible [mm]

The permitted elastic deformation:

$$y_e = \left[0.37 + \sqrt{\frac{300 - V}{1500}} - 0.04 \log G\right] 10 \text{ [mm]}$$

Setting in case of multilayer structure:

$$y = p\left[\frac{f_1}{E_1} + \frac{f_2}{E_2} + \ldots + \frac{f_i}{E_i} + \ldots + \frac{f_n}{E_n}\right] \text{[mm]}$$

and

$$y = \frac{p}{E_e} f$$

$$E_e = \frac{f}{\frac{f_1}{E_1} + \frac{f_2}{E_2} + \ldots + \frac{f_i}{E_i} + \ldots + \frac{f_n}{E_n}} \text{[N/mm}^2\text{]}$$

4.6 Vibration and noise measurements in the track

4.6.1 *Vibration measurements*

At five places of the r.c. slab track of two kinds of foundation and of different times of construction measurements of vibrations caused by vehicles

have been undertaken. At each of the five places four points of measurement were installed. The measurements have been performed under the passage of articulated tram coaches running with 50 and 60 km/h.

The results of the vibration measurements, associated with the speed 50 km/h are summarized in Table 15.

From the data of this table no relations can be established between the age and the movements of the track. A track faultlessly constructed, independently of the foundation method can carry the traffic of 4—5 years without any danger of damage. The displacements of the middle part and corners of the panels show opposite tendencies. On tracks supported on crushed stone bedding the movements of the panel corners are larger than the displacements of the middle parts of the panels. In case of the panels supported on concrete bedding the movements are just the opposite. Accordingly, damaging of the r.c. slab tracks supported on crushed stone bedding takes place at the ends of the panels, the deficiencies of the support present themselves firstly here.

4.6.2 *Noise measurements on the track*

The measurement of the noise has been performed at all of the five measurement places at distances to the track centre line 1.5 m, 5 m and 7.5 m, at a height 1.6 m. The noise level has been measured repeatedly at different speeds. To the measurements a precision device of Bruel and Kjaer production type 2203 has been applied.

The scatter of the results of the noise measurements within each of the measurement places and speed ranges remained, in general, within the permissible value, however, between the places of measurements significant differences occurred.

In Fig. 53 the results of measurements made at the very same place processed are demonstrated from which is to be seen that the noise level expressed in dB(A) is rather the function of the age of the track and not of the method of foundation.

4.6.3 *Noise measurements in the vehicle*

Subsequent to the noise level measurements in the track and along the track measurements were carried out in vehicle, namely in the tram train 1409. Through the noise measurements performed in the tram coach one could not conclude to the kind of foundation of the track. The noise in the coach depends rather on the conditions of the coach and the track as well as on the conditions of the environment (on building density, number of travellers, suspension of the body of vehicle and wheels, etc.) and not on the foundation layers of the track.

4.7 Electrical measurements on the track

The electrical measurements had a double objective;

— The applicability of r.c. track slabs in circuits of insulated rails sections.

— The traction stray current developed due to the construction of track has been investigated.

To the investigation two panels, *640 mm long each* were available in the *laboratory for building industry of the technical University*, measurements have been performed in the street Bécsi út during track laying, on large panels of 6.00 m length as on *panels 6.00 m long. taken from the store of used track slabs withdrawn from the tracks laying in the street Kerepesi út.*

Under the given circumstances the following measurements could be undertaken.

a) Insulation measurement by using d.c. bridge.

b) Resistance measurement with the aid of the method volt/ampere.

c) Earth-resistance measurement using a. current.

d) Insulation-impedance measurement using generator of 13 kHz.

e) Measurement of discharge current and return voltage by applying electronic instrument.

In our investigation work we used also the results of similar research investigations of the railway research institute of *Prague*. In the laboratory, the resistance measurements have been conducted with the aid of the methods a) and b).

The field examinations have been carried out on r.c. slabs of dry, snowy and salted surface.

In summarizing the results of our research investigations we make the following *statements and suggestions.*

The track on large panels and with block rails seems, due to the rubber-strip rail-fastening, to the naked eye to be suitable for producing insulated rail circuits, since no metallic fastening elements come into contact with the rails. The resistance values measured under dry circumstances confirm undoubtedly under certain conditions this assumption. However, the measurements pointed out also the fact that the *resistance values of the rail fastening with rubber strips show even under dry conditions a rather large scatter.* But the resistance values of the track *wetted or covered with salty snow can reduce to 1 or 2 per cent* of that measured at dry state of the track structure.

The panel track structure, compared with that of the state railway main lines with tracks built with r.c. sleepers is, by all means, looking from the viewpoint of the insulated rail-ballast-resistor values, disadvantageous. Considering a spacing of sleepers 70 cm, and a width of sleeper 20 cm, in case of an identic rail fastening, a resistance lower by $70/20 = 3.5$ times is obtained due to the continuous fastening with rubber strips.

The ballast-resistance of 1 ohm · km still tolerated would be accordingly $1/3.5 = 0.286$ ohm · km. Therefrom it follows that the specific contact resistance of the rail fastening has to be elevated to a higher level than that measured on a track supported by r.c. sleepers, further, the lengths of the insulated block rails should be shorter than that applied on railways of distance traffic which, due to the shorter trains, can be realized.

The resistance values are unfavourably influenced also by the *polarization voltage* wich, due to the rubber elements applied continuously along the block rail at its full length, can store higher energy than the r.c. sleepers, wherefore, it is to be feared that in case of using d.c. rail circuits, defective phenomena can cause which are not expected.

From the above said is to be concluded that the *present structure of the large-panel track is not suitable to establish on the tramway lines insulated rail circuits.*

From the viewpoint of the *stray currents more favourable statements can be made* on the basis of measurement results obtained in the examinations mentioned above. The quality of the insulation of the large panels may depend in a large extent on the quality of the bituminous and crushed stone foundation and on the water content of the soil. However, a final statement cannot be made with appropriate safety due to the measurements which could be performed under the actual conditions.

4.8 Further examinations

In the course of the research investigation undertaken by the Department of Railway Construction a few further details have been handled. Suggestions have been worked out to the lateral support of the block rail in order to reduce the frequency of occurrence of the deficiencies of the alignement and gauge, to assure the connection and coaction of the adjoining track slabs since between them currently only the block-rail constitutes a connection. Finally to the toleration in measurements of the track elements and the block-rail as well as to the rules of their delivery and acceptance a draft has been worked out. These examinations of structural character are here not discussed.

Summary and suggestions

Summarizing the results of the research investigation work carried out by the Department of Railway Construction we make the following *statements and suggestions.*

1) The compression stresses induced in the *block rails* by vertical bending are higher than those arisen in the tramway rail Phoenix but remain under

the stress values induced in the rails of the national railways. The critical *tensile stresses* as well as the *Hertzian contact strength* in case of rails of 7000 daN/cm^2 tensile strength surpass the permissible stress values, therefore, I suggest to *augment the minimum value of the tensile strength of the block rail to 8000 daN/cm^2.*

2) To the design of the *insulation joints* of the block rails proposal has been made mentioned here earlier.

3) To the up-to-date dimensioning of the *track slab* a computerized *calculation method* has been worked out; I suggest its application in the course of further development.

4) The *bending tests carried out on the r.c. track slabs* resulted, in spite of extraordarily unfavourable support conditions at all tests in a load of failure higher than the critical loading of the road vehicle used for basis to the dimensioning. The tests pointed out that the slabs can resist the loading of the road vehicles with a high safety without suffering any damages.

5) The *surface roughness* of the track slabs, according to the roughness tests performed as is prescribed by the standard on the subject, is satisfactory.

6) The *stability* of the *r.c. trak slab laid* in the track is *equally satisfactory both in respect to the vertical and horizontal buckling of the track.*

7) *A vertical displacement* of the finished track structure with its integrated *block rail* — according to the calculations performed — *cannot take place* in the case where the final welding is carried out above the $+5$ °C rail temperature. During construction if *no tensioning rubber strip is yet laid with the block rails*, already an increase in rail temperature $\Delta t = 15$—20 °C can cause rail displacement.

8) In the track structure constructed, the reitaration of *road vehicle loading can induce movement and jam of the track slabs.* For augmenting the stability, it is advisable to apply either structural elements increasing the friction or slab anchorages.

9) Slip of the *track slabs downwards on the gradients of the track* being under operation has no significance.

10) The *rubber strip fastening of the block rails* is, looking from the viewpoint of resisting the vertical and horizontal rail movements is *satisfactory.*

11) *For the pression of the rubber strip* into the rail seat, the method to *proceed in sections* suggested in Chapter 4.4 is advisable.

12) In the course of detailed theoretical and experimental investigations the characteristics of *four* different *bedding designs* have been compared and qualified. In our opinion to develop the track system in question *mortar-like substances are the* most appropriate.

13) From the *vibration measurements* performed in the track no relations could be found between the service age of the track and vibration.

14) The *noise measurements* performed on the track and in the vehicles showed that the noise induced depended rather on the type of vehicle, the en-

vironment and the age of the track and not on the two different foundation system (i.e. crushed stone and concrete layer).

15) The track system is *unsuitable* for producing *insulated rail circuits.*

16) It is advisable to render more severe the tolerances on the dimensions of the r.c. track slabs, however, the new tolerance values should be brought into harmony with the designs of the foundation and the subgrade.

On commission of the Budapest Transport Company as well as the Concrete and R.C. Industrial Works, the Department of Railway Construction of the Technical University of Budapest performed a *particularly extensive research investigation.* Such an overall, extensive research investigation of a new railway superstructure is of a pioneering character, for the initiation of which grateful acknowledgements are due to the employers.

As a final conclusion of the three years' conclusion can be drawn that the r.c. track slab system with block rails designed by the BKV—*Budapest Transport Company* and the BVM — Concrete and R.c. Works

— has been created as a result of a *careful engineering and economical study,*
— performs its function without accidents and without the danger of buckling,
— the tracklaying of which can be mechanized to a great extent,
— its *rail fastening* of new design is advantageous both from the point of view of the tracklaying work and from the service concerning both the engineering and economical requirements,
— in summing up, considering the conditions of track maintenance of the Budapest tramway network, the track construction in question may be considered a *well proved track design.*

For completing and developing the extensive research investigation the Department for Railway Construction *deems with the view of further improvement of the track system in question to be advisable to carry out the following research investigation:*

a) A strengthened r.c. track slab and foundation should be designed for *level crossings* of roads with dense transverse road traffic.

b) A more economical design of r.c. track slab should be applied for sections on which *no road traffic takes place.*

c) Testing, i.e. applying an *injected grout bedding is advisable.*

d) A theoretical study on the development of the block rail profile should be undertaken mainly on the thickening of the guard lip of rail and on the revision of the measurement tolerances of the rail flange.

e) The length, now 6.00 m of the r.c. track slab should incidentally be altered considering the swinging of the vehicles. A study would be advisable for clearing up this question.

f) Considering also the Chechoslovakian investigations a study on the improvement of the surface shaping of the r.c. track slabs should be undertaken.

g) A study on the structural and geometrical design of turnouts and crossings of block rail tracks also should be undertaken.

h) The causes of the rapid smashing of the rail channel in the slab and the prevention of this phenomenon should be examined.

This study is intended to give an overall survey on the extensive research investigation performed at the Department for Railway Construction of the Technical University Budapest in connection with the track structure built with block rails on r.c. slabs for the Budapest tramway and summarizes the material of the 10 reports on the research investigation of an extent of 712 typescript pages summarized in the present paper.

The author endeavoured to adhere to a moderate extent in order to make easier the use of this paper by neglecting calculation details and shortening the description of the tests carried out. His objective was, among others, to present the test results the details of which are otherwise to be found in the interim reports of the work.

The research investigation has been performed under the leadership of *Endre Kerkápoly*, Professor, Head of Department, by *Attila Horváth*, *Károly Kurutz*, and *István Szatmári* associate professors, *Tibor Kósa*, *György Molnár* and *János Székely* senior assistants, *Ferenc Fazekas* and *László Kazinczy* assistants with the efficacious collaboration of the whole staff of the railway track laboratory of the Department.

References

The research investigation reports of the Department for Railway Construction T. U. Budapest:

1. Stability examination of the large-panel tramway track construction, 234002/1974, October 1974.
2. Slip tests on the block rail track slab, 234507/1975, September 1975.
3. Examination of the block rail of the large panel track, 234005/1980, November 1980.
4. Technical and constructional data. Electric measurements, 234004/1980, January 1981.
5. Laboratory tests on the rail fastening, 234005/1980, January 1981.
6. Noise and swinging tests. Impression tests of the rubber strip, 234003/1980, December 1981.
7. Tests on the reinforced concrete slab: A. Failure tests on the track slabs VL-60. B. Realization of the cooperation of the track slabs, 234007/1980, February 1982.
8. Surface roughness of the prefabricated track slabs. Acceptance specification of the r.c. track slab and the block rail, 234007/1980, July 1982.
9. Foundation problems of the r.c. track slab system, 234006/1980, November 1982.
10. Problems of dimensioning of the system of the prefabricated r.c. track slab, 234007/1980, November 1982.

Prof. Dr. Endre KERKÁPOLY H-1521 Budapest